IEEE Access
Multidisciplinary | Rapid Review | Open Access Journal

Received April 7, 2021, accepted May 19, 2021, date of publication May 28, 2021, date of current version June 8, 2021.

Digital Object Identifier 10.1109/ACCESS.2021.3084627

A Nonuniform-Quantized Successive Cancellation Decoding of Polar Codes Over AWGN Channels

JIHO KIM, (Member, IEEE), AND DONG-JOON SHIN, (Senior Member, IEEE)
Department of Electronic Engineering, Hanyang University, Seoul 04763, South Korea

Corresponding author: Dong-Joon Shin (djshin@hanyang.ac.kr)

This work was supported by the Korea Institute for Advancement of Technology (KIAT) Grant by the Korean Government [Ministry of Trade, Industry and Energy (MOTIE)] through the Human Resources Development (HRD) Program for Industrial Innovation under Grant P0017011.

ABSTRACT Since polar codes are capacity-achieving codes, there have been various research works devoted to devising efficient implementation methods as well as improving error-correction performance. Since quantization is a critical implementation issue, in this paper, a nonuniform quantization method is proposed for the successive cancellation (SC) decoder of polar codes, which finds quantization boundary values based on the analysis of various quantization levels over the additive white Gaussian noise channel. Since low computational complexity, high reliability, and efficient memory management are required in the next-generation communication and memory systems, 2-4 bit precision levels are mainly considered in the proposed nonuniform quantization method. Depending on the presence of erasure, quantization levels are divided into three types, and the message alphabets and update rules are derived for each type. Also, a construction method of polar codes suitable for the proposed nonuniform-quantized SC decoder is proposed, which simultaneously determines the information set and the quantization boundary values based on the density evolution analysis and an upper bound of the block error probability. To determine quantization boundary values, a multivariate objective function is defined and an iterative coarse-to-fine search algorithm to minimize this objective function is proposed. In addition, a scaling method of quantizer output values is proposed when the number of quantization levels of quantizer is smaller than the number of quantization levels of decoder. Finally, simulation results confirm that the proposed nonuniform-quantized SC decoder shows better error-correction performance, lower decoding complexity, and higher memory efficiency compared to the best known uniform-quantized SC decoder.

INDEX TERMS Block error probability, density evolution, iterative coarse-to-fine search algorithm, minimization problem, nonuniform quantization, polar codes, successive cancellation decoding.

I. INTRODUCTION

It is well known that polar codes achieve the capacity of any symmetric binary-input discrete memoryless channel (B-DMC) with an explicit construction [1]. They are based on channel polarization which refers to the fact that it is possible to synthesize N independent copies of a given B-DMC by performing channel combining and splitting. As N goes to infinity, the N synthesized channels are constructed such that some of them are noiseless and the remaining ones are completely unreliable, and the fraction of the noiseless channels approaches the symmetric capacity of the given B-DMC. Therefore, by transmitting information bits through the noiseless channels and frozen bits (fixed bits) through the remaining unreliable channels, polar codes can achieve the symmetric capacity under a successive cancellation (SC) decoding when N is large enough [1].

However, for a finite code length, polar codes tend to show worse error-correction performance compared to other conventional coding schemes [2]. For this reason, there have been intense research works devoted to improving the decoding performance such as SC list (SCL) decoding [3], [4], and SC stack (SCS) decoding [5]. For practical applications, improved architectures of SC decoding have been discussed in [6]–[11] and polar codes were selected to protect the control channels in the 3rd Generation Partnership Project New Radio candidate for the fifth generation (5G) mobile communications [12], [13]. In 5G mobile communications

The associate editor coordinating the review of this manuscript and approving it for publication was Cristian Zambelli.

and Internet of Things (IoT), high error-correction capability, low computational complexity, and efficient memory management are required, and various polar coding and decoding schemes have been studied to satisfy these requirements [14]–[19]. Also, in memory systems such as NAND flash memory, applications of polar code have been studied due to the low encoding/decoding complexity and the flexibility of the code rate of polar codes [20], [21]. However, soft-decision polar decoding requires fine-grained threshold-voltage sensing operation [22] and hence incurs penalties in energy consumption and access latency. Therefore, it is important to minimize the number of threshold-voltage sensing operations without serious degradation of error-correction performance. The number of threshold-voltage sensing operations is proportional to the number of quantization levels for quantizer.

In the next-generation communication and memory systems, quantization is a critical issue in hardware implementation. The robustness of quantized SC decoding was analyzed in [23] but any specific quantization scheme was not proposed. In [24], the performance of short polar codes under SC and SCL decoding was analyzed when the decoder messages are quantized with 3 levels. By using the information bottleneck method, a design method of discrete SCL decoder was proposed in [25]. As a practical quantization scheme, an optimized uniform quantization method for SC decoder was proposed in [26], which is based on the minimum mean-squared error quantization, capacity-maximizing criterion, and cut-off rate maximizing criterion. However, quantization should be performed for each node operation and the messages updated by uniform-quantized SC decoder take fixed-point numbers. In addition, quantization boundary (QB) values are stored as many as the number of nodes since quantization is performed for each node.

In this paper, a nonuniform quantization method (NQM) and a nonuniform-quantized SC (NQSC) decoding algorithm of polar codes are proposed. Quantization is mostly focused on $2, 3, 4$-bit precision levels because low bit precision is particularly useful for applications that require energy efficient transceivers with low computational complexity such as NAND flash memory, IoT, and wireless sensor networks [22], [24], [27]. Specifically, NQMs are proposed for the cases where the number of quantization levels of quantizer is equal to or smaller than the number of quantization levels of decoder. Note that if the latter is applied to the memory systems, the number of threshold-voltage sensing operations can be reduced without noticeable error-correction performance degradation. Depending on the number of quantization levels and the presence of erasure, the quantization levels are divided into three types: (i) symmetric odd quantization levels, (ii) asymmetric even quantization levels, and (iii) symmetric even quantization levels. According to the type of quantization levels, both the message alphabets for quantizer and quantized SC decoder are determined and the message update rules suitable for the proposed quantized SC decoding are also determined.

Unlike uniform quantization methods, which determine the quantization boundary values by using a constant quantization interval, it is a difficult problem for NQMs to determine all the quantization boundary values. In this paper, an upper bound (UB) of block error probability (BEP), which is derived through density evolution analysis by using the QB values as its arguments, is derived as a multivariate objective function, and an iterative coarse-to-fine (C2F) search algorithm is proposed to minimize this complicated objective function. Through the proposed search algorithm, the QB values and the information set are obtained simultaneously. The computational complexity of the proposed iterative C2F search algorithm is compared to that of a trivial exhaustive search algorithm. Also, for the case that the number of quantization levels of quantizer is smaller than the number of quantization levels of quantized SC decoder, a scaling method is proposed to match the maximum and minimum quantization levels of quantizer to those of quantized SC decoder.

The performance of the proposed NQSC decoder is compared with that of the existing quantized SC decoder through simulations under additive white Gaussian noise (AWGN) channels. Simulation results confirm that the proposed NQM for SC decoder outperforms the optimal uniform quantization method in [26]. Also, the proposed NQSC decoding algorithm has lower decoding complexity and higher memory efficiency compared to the optimal uniform-quantized SC decoder in [26] by the following reasons: (i) the proposed decoding algorithm does not perform quantization for each node operation, (ii) the messages updated by the proposed decoding algorithm are not fixed-point numbers but integers, and (iii) the number of QB values to be stored is small. Through simulations, the effect of erasure on the error-correction performance according to the number of quantization levels and signal-to-noise ratio (SNR) is analyzed. It is also confirmed that error-correction performance of quantized SC decoder is improved by increasing the number of its quantization levels while keeping the number of quantization levels of quantizer fixed. Finally, it is discussed how to reduce the decoding latency and the number of reading operations in communication and memory systems by setting the number of quantization levels for each of quantizer and decoder differently.

The rest of the paper is organized as follows. In Section II, the basics of polar codes are briefly explained. Section III introduces the system model, quantization schemes for quantizer and quantized SC decoder, and update rules of quantized message values for quantized SC decoding. In Section IV, an NQM and a quantized SC decoding method based on density evolution analysis are proposed, deriving an UB of BEP, and applying an iterative C2F search algorithm. Simulation results are provided in Section V and the conclusions are given in Section VI. Finally, in Section VI, it is also discussed how to reduce the decoding latency and the number of reading operations in communication and memory systems.

II. POLAR CODES

In this section, basic notations for polar codes are defined, channel combining and splitting for channel polarization phenomena are introduced, and the encoding and SC decoding schemes of polar codes are explained.

A. NOTATIONS

A B-DMC is denoted by $W : \mathcal{X} \to \mathcal{Y}$ with the input alphabet $\mathcal{X} = \{0, 1\}$, the output alphabet $\mathcal{Y}$, and the channel transition probabilities $W(y|x)$ where $x \in \mathcal{X}$ and $y \in \mathcal{Y}$. For the block length $N = 2^n$ with $n \geq 0$, we consider an $N \times N$ generator matrix $G_N \triangleq P_N A^{\otimes n}$ where $A \triangleq \left[\begin{smallmatrix} 1 & 0 \\ 1 & 1 \end{smallmatrix}\right]$, P_N is the $N \times N$ bit-reversal permutation matrix, and $(\cdot)^{\otimes n}$ denotes the nth Kronecker power [1]. Let $\mathbf{u} = u_0^{N-1} = (u_0, u_1, \cdots, u_{N-1})$ be an input vector of length N, $\mathbf{x} = x_0^{N-1} = (x_0, x_1, \cdots, x_{N-1}) = \mathbf{u}G_N$ be a codeword of length N for $\mathbf{u}$, and $\mathbf{y} = y_0^{N-1} = (y_0, y_1, \cdots, y_{N-1})$ be the corresponding received vector of length N. Here, $u_i \in \mathcal{U} = \{0, 1\}$ and $\mathcal{U}$ is the binary input alphabet of encoder. W^N denotes the N independent copies of B-DMC W, and $W^N : \mathcal{X}^N \to \mathcal{Y}^N$ denotes the channel model with the transition probabilities $W^N(\mathbf{y}|\mathbf{x}) = \prod_{i=0}^{N-1} W(y_i|x_i)$.

B. CHANNEL COMBINING AND SPLITTING

Channel polarization implies that it is possible to synthesize N binary-input channels by performing channel combining and to divide this synthesized channel back into noisy and noiseless channels by performing channel splitting. Through the recursion of combining two independent copies of W, N independent channels W^N are combined into a channel $W_N : \mathcal{U}^N \to \mathcal{Y}^N$ and then split into N binary-input channels $W_N^{(i)}$, $0 \leq i \leq N-1$, as follows.

First, set $W_1 \triangleq W$. Then, two independent copies of W_1 are combined to create the channel $W_2 : \mathcal{U}^2 \to \mathcal{Y}^2$ with the transition probabilities $W_2(y_0^1|u_0^1) = W_1(y_0|u_0 \oplus u_1)W_1(y_1|u_1)$ where $\oplus$ is the modulo-2 addition. Next, two independent copies of W_2 are combined to create the channel $W_4 : \mathcal{U}^4 \to \mathcal{Y}^4$ with the transition probabilities $W_4(y_0^3|u_0^3) = W_2(y_0^1|u_0 \oplus u_1, u_2 \oplus u_3)W_2(y_2^3|u_1, u_3)$. By repeating this recursive combining operation up to n times, $W_{2^j}(y_0^{2^j-1}|u_0^{2^j-1}) = W_{2^{j-1}}(y_0^{2^{j-1}-1}|u_0 \oplus u_1, u_2 \oplus u_3, \cdots, u_{2^j-1} \oplus u_{2^j})W_{2^{j-1}}(y_{2^{j-1}}^{2^j-1}|u_1, u_3, \cdots, u_{2^j})$, $1 \leq j \leq n$, are obtained and the synthesized channel W_N is created where $N = 2^n$, that is called channel combining. Then, the transition probabilities of two channels W_N and W^N are related by $W_N(\mathbf{y}|\mathbf{u}) = W_N(y_0^{N-1}|u_0^{N-1}) = W^N(y_0^{N-1}|u_0^{N-1}G_N) = W^N(\mathbf{y}|\mathbf{x})$. Given the synthesized channel W_N, it can be split back into a set of N binary-input coordinate channels $W_N^{(i)} : \mathcal{U} \to \mathcal{Y}^N \times \mathcal{U}^i$ for $0 \leq i \leq N-1$. The transition probabilities of these coordinate channels are derived as $W_N^{(i)}(y_0^{N-1}, u_0^{i-1}|u_i) = \sum_{u_{i+1}^{N-1} \in \mathcal{U}^{N-i-1}} \frac{1}{2^{N-1}} W_N(y_0^{N-1}|u_0^{N-1})$ [1].

C. ENCODING

Let K and $R = K/N$ be the number of information bits and the code rate, respectively. As N increases, the capacity of each coordinate channel $I(W_N^{(i)})$ for $0 \leq i \leq N-1$ approaches either 1 (noiseless channel) or 0 (noisy channel). It is well known that the fraction of these noiseless channels approaches the symmetric capacity of the underlying channel W. For $\mathcal{S} \subseteq \{0, 1, \ldots, N-1\}$ and $|\mathcal{S}| = K$, the information set $\mathcal{I}$ is defined as $\mathcal{I} = \arg\max_{\mathcal{S}} \sum_{i \in \mathcal{S}} I(W_N^{(i)})$ and an input vector $\mathbf{u}$ can be divided into two parts as $\mathbf{u} = (\mathbf{u}_{\mathcal{I}}, \mathbf{u}_{\mathcal{I}^c})$ where $\mathbf{u}_{\mathcal{I}} = (u_i : i \in \mathcal{I})$ consists of K information bits and $\mathbf{u}_{\mathcal{I}^c} = (u_i : i \in \mathcal{I}^c)$ consists of $N-K$ fixed constant values (usually 0) which are called frozen bits. Then, an input vector $\mathbf{u}$ is encoded to $\mathbf{x} = \mathbf{u}_{\mathcal{I}}G_N(\mathcal{I}) \oplus' \mathbf{u}_{\mathcal{I}^c}G_N(\mathcal{I}^c)$ where $\oplus'$ is the modulo-2 vector addition and $G_N(\mathcal{T})$ denotes the submatrix of G_N formed by the rows with the indices from the set $\mathcal{T}$.

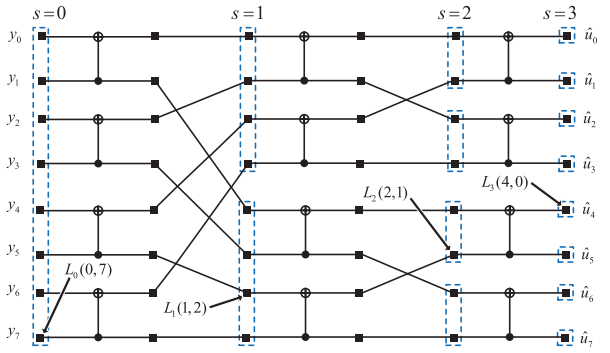

FIGURE 1. Factor graph of SC decoder for $N = 8$.

D. SUCCESSIVE CANCELLATION (SC) DECODING

An SC decoding for polar codes was proposed by E. Arıkan [1], which is a capacity-achievable decoding when N is large enough. In this section, notations and descriptions of SC decoding are given as in [3], [28]. SC decoder operates on a factor graph of polar codes. The factor graph of polar codes consists of $N(n+1)$ nodes and can be divided into $n+1$ columns, where each column of the factor graph is indexed with $s \in \{0, 1, \cdots, n\}$. Each column consists of 2^s groups indexed by $\phi \in \{0, 1, \cdots, 2^s - 1\}$ where each group consists of 2^{n-s} nodes indexed by $\omega \in \{0, 1, \cdots, 2^{n-s} - 1\}$. For example, if $N = 8$, the factor graph has two node groups under $s = 1$, i.e., the upper group and the lower group represented by $\phi = 0$ and $\phi = 1$, respectively. The nodes within each of these node groups are indexed by $\omega \in \{0, 1, 2, 3\}$. Fig. 1 shows the factor graph of SC decoder for $N = 8$, where the dashed boxes represent groups. Let $L_s(\phi, \omega)$ be the log-likelihood ratio (LLR) and $B_s(\phi, \omega)$ be the bit-decision (0 or 1) of the node ω in the node group ϕ at the stage s of the graph, which is computed from detected/known bits. Hereafter, the bit-decision $B_s(\phi, \omega)$ is represented as an LLR form such as $0 \to \infty$ and $1 \to -\infty$. At the receiver having the fact that frozen bits $\mathbf{u}_{\mathcal{I}^c}$ are fixed as 0, the information set $\mathcal{I}$, and the received vector $\mathbf{y}$, the SC decoder performs an estimation $\hat{u}_0^{N-1}$ of u_0^{N-1}, which is done as

$$\hat{u}_i \triangleq \begin{cases} 0, & \text{if } i \in \mathcal{I}^c \text{ or } B_n(i, 0) > 0 \\ 1, & \text{otherwise} \end{cases} \tag{1}$$

Algorithm 1: SC Decoding

$\{L_0(0,i)\}_{i=0}^{N-1} \leftarrow$ LLRs from channel
$\{B_n(i,0)\}_{i\in\mathcal{I}^c} \leftarrow \infty$, $\{B_n(i,0)\}_{i\in\mathcal{I}} \leftarrow 0$
for $\phi = 0 \rightarrow N-1$ **do**
  UpdateLLRMap(n,ϕ)
  if $\phi \in \mathcal{I}$ **then**
    if $L_n(\phi,0) \geq 0$ **then**
      $B_n(\phi,0) \leftarrow \infty$
    else
      $B_n(\phi,0) \leftarrow -\infty$
  if ϕ is odd **then**
    UpdateBitMap(n,ϕ)
for $i = 0 \rightarrow N-1$ **do**
  if $i \in \mathcal{I}^c$ or $B_n(i,0) > 0$ **then**
    $\hat{u}_i \leftarrow 0$
  else
    $\hat{u}_i \leftarrow 1$

for $i = 0, 1, \cdots, N-1$ where $B_n(i,0)$ is the LLR value of $B_s(\phi,\omega)$ when $s = n$, $\phi = i$, and $\omega = 0$. The input LLRs $L_0(0,i)$ and the bit-decisions $B_n(i,0)$ for $i = 0, 1, \ldots, N-1$ are initialized as

$$L_0(0,i) = \log\frac{\Pr(x_i = 0|y_i)}{\Pr(x_i = 1|y_i)} \tag{2}$$

and

$$B_n(i,0) = \begin{cases} \infty, & \text{if } i \in \mathcal{I}^c \\ 0, & \text{otherwise.} \end{cases} \tag{3}$$

Here, $B_n(i,0)$ is 0 when $i \in \mathcal{I}$ because there is no information about $\mathbf{u}_\mathcal{I}$ in the initialization stage of SC decoding. For $i = 0, 1, \cdots, N-1$, $L_n(i,0)$ is sequentially computed by the recursion

$$L_s(\phi,\omega) = L_{s-1}(\psi, 2\omega) \odot L_{s-1}(\psi, 2\omega+1) \tag{4}$$

for even ϕ and

$$L_s(\phi,\omega) = L_{s-1}(\psi, 2\omega+1) + L_{s-1}(\psi, 2\omega) \odot B_s(\phi-1,\omega) \tag{5}$$

for odd ϕ. Here, $\odot$ is defined as $a \odot b \triangleq 2\tanh^{-1}\left[\tanh(a/2) \times \tanh(b/2)\right]$ and $\psi = \lfloor \frac{\phi}{2} \rfloor$ where $\lfloor a \rfloor$ denotes the largest number of integers equal to or less than a. Whenever $L_n(i,0)$ is computed for each $i \in \mathcal{I}$, $B_n(i,0)$ is updated by

$$B_n(i,0) = \begin{cases} \infty, & \text{if } L_n(i,0) \geq 0 \\ -\infty, & \text{otherwise.} \end{cases} \tag{6}$$

Also, whenever $L_n(i,0)$ is updated for odd values of i, $B_s(\phi,\omega)$ are updated by

$$\begin{aligned} B_{s-1}(\psi, 2\omega) &= B_s(\phi-1,\omega) \odot B_s(\phi,\omega) \\ B_{s-1}(\psi, 2\omega+1) &= B_s(\phi,\omega) \end{aligned} \tag{7}$$

where $\psi = \lfloor \frac{\phi}{2} \rfloor$.

The pseudo codes of the SC decoding algorithm are presented as Algorithms 1-3. Algorithm 1 is the main algorithm of SC decoding, and bit-decision and LLR of each node are updated in Algorithms 2 and 3, respectively.

Algorithm 2: UpdateBitMap (s,ϕ)

if ϕ is odd **then**
  for $\omega = 0 \rightarrow 2^{n-s} - 1$ **do**
    $B_{s-1}(\psi, 2\omega) \leftarrow B_s(\phi-1,\omega) \odot B_s(\phi,\omega)$
    $B_{s-1}(\psi, 2\omega+1) \leftarrow B_s(\phi,\omega)$
  if ψ is odd **then**
    UpdateBitMap$(s-1,\psi)$

Algorithm 3: UpdateLLRMap (s,ϕ)

if $s = 0$ **then**
  return $\psi \leftarrow \lfloor \frac{\phi}{2} \rfloor$
if ϕ is even **then**
  UpdateLLRMap$(s-1,\psi)$
for $\omega = 0 \rightarrow 2^{n-s} - 1$ **do**
  if ϕ is even **then**
    $L_s(\phi,\omega) \leftarrow L_{s-1}(\psi, 2\omega) \odot L_{s-1}(\psi, 2\omega+1)$
  else
    $L_s(\phi,\omega)$
    $\leftarrow L_{s-1}(\psi, 2\omega+1) + L_{s-1}(\psi, 2\omega) \odot B_s(\phi-1,\omega)$

III. SYSTEM MODEL AND MESSAGE UPDATE RULES FOR QUANTIZATION SCHEMES

This section first describes the transmitted signal, received signal, and channel model. Next, quantization schemes for quantizer and quantized SC decoder according to the type of quantization levels are presented. Finally, message update rules for quantized SC decoding are explained according to the type of quantization levels.

A. SYSTEM MODEL

Let $\mathbf{v} = v_0^{N-1} = (v_0, v_1, \cdots, v_{N-1})$ be a binary phase shift keying (BPSK) modulated vector of a binary codeword $\mathbf{x}$ where $v_i = (-1)^{x_i} \in \{1, -1\}$. The vector $\mathbf{v}$ is transmitted and $\mathbf{y}(= \mathbf{v}+\mathbf{n})$ is received at the receiver through AWGN channel where $\mathbf{n} = n_0^{N-1} = (n_0, n_1, \cdots, n_{N-1})$ is a noise vector. The noise elements n_i are independent and identically distributed, which are drawn from the zero-mean Gaussian distribution with variance σ^2, represented as $n_i \sim \mathcal{N}(0,\sigma^2)$. SNR in dB scale is denoted by γ and is calculated as $\gamma = \text{SNR[dB]} = E_b/N_0\ \text{[dB]} = 10\log_{10}(E_b/N_0) = 10\log_{10}((E_c/R)/N_0)) = 10\log_{10}(1/(2\sigma^2 R))$ where E_b denotes the energy per information bit, E_c denotes the energy per codeword bit which is fixed to 1, and $N_0/2(=\sigma^2)$ denotes the noise power spectral density.

B. QUANTIZATION SCHEMES FOR QUANTIZER AND QUANTIZED SC DECODER ACCORDING TO THE TYPE OF QUANTIZATION LEVELS

Let Q and q be the number of quantization levels for quantizer and quantized SC decoder, respectively. Note that a quantization level denotes a single value representing all values

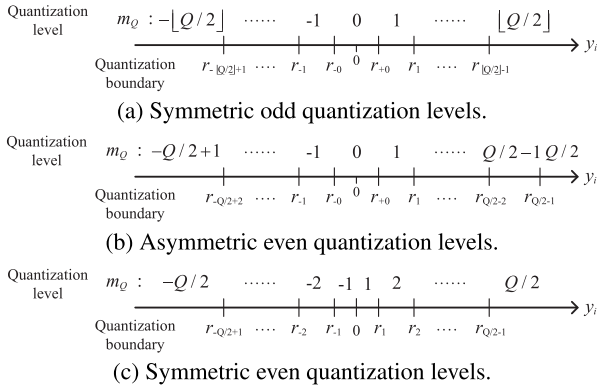

FIGURE 2. Three types of quantization levels.

contained in the corresponding quantization interval. The sign of the quantization level indicates whether a transmitted BPSK modulated symbol is estimated to be -1 or $+1$ and the absolute value of the quantization level is a measure of the reliability of this estimate [29]. Each real value y_i of the received vector $\mathbf{y}$ is quantized into one of Q quantization levels and such quantized received vector is decoded by the q-level quantized SC decoder, which performs decoding using the messages expressed by q quantization levels.

Fig. 2 shows three types of quantization levels: (i) symmetric odd quantization levels, (ii) asymmetric even quantization levels, and (iii) symmetric even quantization levels. Here, r_k denotes QB value and the quantization level for the quantization interval $[r_{-0}, r_{+0}]$ is 0 which is called erasure. Figs 2(a) and (b) show symmetric odd and asymmetric even quantization levels with erasure, respectively. On the other hand, as shown in Fig. 2(c), symmetric even quantization levels do not include erasure. Symmetric odd and even quantization levels were used in [29]. The type of asymmetric even quantization levels is obtained by adding one quantization level to the symmetric odd quantization levels. To confirm the error-correction performance according to the presence of erasure, even quantization levels are divided into the cases with and without erasure, and the error-correction performances for these cases are compared in Section V. If Q is an odd number, $\mathcal{M}_Q = \{-\lfloor Q/2 \rfloor, \cdots, -1, 0, 1, \cdots, \lfloor Q/2 \rfloor\}$ where $\mathcal{M}_Q$ and $m_Q \in \mathcal{M}_Q$ denote the message alphabet for the quantizer outputs and the output symbol of the quantizer, respectively, and y_i is quantized to the symbol m_Q by the following quantization function

$$f_Q(y_i) = \begin{cases} -\lfloor Q/2 \rfloor, & \text{if } -\infty < y_i < r_{-\lfloor Q/2 \rfloor+1} \\ \vdots & \\ -1, & \text{if } r_{-1} \le y_i < r_{-0} \\ 0, & \text{if } r_{-0} \le y_i \le r_{+0} \\ 1, & \text{if } r_{+0} < y_i \le r_1 \\ \vdots & \\ \lfloor Q/2 \rfloor, & \text{if } r_{\lfloor Q/2 \rfloor-1} < y_i < \infty. \end{cases} \tag{8}$$

Next, if Q is an even number and erasure is included in the quantization levels, i.e., asymmetric even level quantization, $\mathcal{M}_Q = \{-Q/2+1, \cdots, -1, 0, 1, \cdots, Q/2\}$ and the quantization function is given as

$$f_Q(y_i) = \begin{cases} -Q/2+1, & \text{if } -\infty < y_i < r_{-Q/2+2} \\ \vdots & \\ -1, & \text{if } r_{-1} \le y_i < r_{-0} \\ 0, & \text{if } r_{-0} \le y_i \le r_{+0} \\ 1, & \text{if } r_{+0} < y_i \le r_1 \\ \vdots & \\ Q/2, & \text{if } r_{Q/2-1} < y_i < \infty. \end{cases} \tag{9}$$

If Q is an even number and erasure is not included in the quantization levels, i.e., symmetric even level quantization, $\mathcal{M}_Q = \{-Q/2, \cdots, -1, 1, \cdots, Q/2\}$ and the quantization function is given as

$$f_Q(y_i) = \begin{cases} -Q/2, & \text{if } -\infty < y_i < r_{-Q/2+1} \\ \vdots & \\ -1, & \text{if } r_{-1} \le y_i < 0 \\ 1, & \text{if } 0 < y_i \le r_1 \\ \vdots & \\ Q/2, & \text{if } r_{Q/2-1} < y_i < \infty. \end{cases} \tag{10}$$

In this paper, we mainly consider the case of $Q = q$, i.e., $\mathcal{M}_Q = \mathcal{M}_q$ where $\mathcal{M}_q$ is the message alphabet for the messages used in the quantized SC decoding. Note that Q does not have to be equal to q. In Section IV, a new NQM is proposed for the cases of $Q = q$ and $Q < q$. We do not consider the case of $Q > q$ because information loss occurs due to insufficient number of quantization levels for SC decoding, which significantly affects the decoding performance.

C. MESSAGE UPDATE RULES FOR QUANTIZED SC DECODER ACCORDING TO THE TYPE OF QUANTIZATION LEVELS

Fig. 3(a) shows a basic structure of polar codes, which consists of one check node and one repetition node with two input bits (u_0, u_1), and two output bits (x_0, x_1) where $u_0, u_1, x_0, x_1 \in \mathcal{M}_q$. Also, Figs 3(b) and (c) show the decoding operations at the check node and at the repetition node, respectively.

At the check node, the output message $m_{\text{out,ch}}$ is determined by two input messages m_0 and m_1 such as $m_{\text{out,ch}} = m_0 \circ m_1$ where the operation $\circ : \mathcal{M}_q \circ \mathcal{M}_q \to \mathcal{M}_q$, called min-approximation [6], [24], is defined as $\alpha \circ \beta = \text{sgn}(\alpha)\text{sgn}(\beta)\min(|\alpha|, |\beta|)$, and $\text{sgn}(t)$ is defined as $t/|t|$ if $t \neq 0$ and 0 if $t = 0$.

At the repetition node, if the signs of two input values are the same, the repetition node operation is defined to determine the value with higher reliability, otherwise it is defined

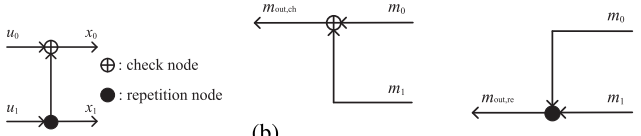

(a) Basic structure of polar codes.

(b) Simplification of check node operation.

(c) Simplification of repetition node operation.

FIGURE 3. Basic structure of polar codes and simplification of decoding operations at the check node and the repetition node for SC decoding.

as the sum of two input values. So, if erasure is contained in q quantization levels, the output message of repetition node $m_{\text{out,re}}$ is determined by two input messages m_0 and m_1 such as $m_{\text{out,re}} = m_0 \star m_1$ where the operation $\star : \mathcal{M}_q \star \mathcal{M}_q \to \mathcal{M}_q$ is defined as

$$\alpha \star \beta = \begin{cases} \alpha, & \text{if } \operatorname{sgn}(\alpha) = \operatorname{sgn}(\beta) \text{ and } |\alpha| \geq |\beta| \\ \beta, & \text{if } \operatorname{sgn}(\alpha) = \operatorname{sgn}(\beta) \text{ and } |\alpha| < |\beta| \\ \alpha + \beta, & \text{otherwise.} \end{cases} \tag{11}$$

On the other hand, if q quantization levels do not contain erasure, the output message of repetition node $m_{\text{out,re}}$ is determined as $m_{\text{out,re}} = m_0 * m_1$ where the operation $* : \mathcal{M}_q * \mathcal{M}_q \to \mathcal{M}_q$ is defined as

$$\alpha * \beta = \begin{cases} \alpha, & \text{if } \operatorname{sgn}(\alpha) = \operatorname{sgn}(\beta) \text{ and } |\alpha| \geq |\beta| \\ \beta, & \text{if } \operatorname{sgn}(\alpha) = \operatorname{sgn}(\beta) \text{ and } |\alpha| < |\beta| \\ \alpha \diamond \beta, & \text{if } \operatorname{sgn}(\alpha) \neq \operatorname{sgn}(\beta) \text{ and } |\alpha| = |\beta| \\ \alpha + \beta, & \text{otherwise} \end{cases} \tag{12}$$

where $\alpha \diamond \beta$ denotes a selection of $\operatorname{sgn}(\alpha)$ or $\operatorname{sgn}(\beta)$ uniformly at random, i.e., random selection of $+1$ and -1 with probability $1/2$.

If q quantization levels for quantized SC decoder do not contain erasure, there is an ambiguity in determining the output message at the repetition node. For example, the output message at the repetition node cannot be determined if two input messages are α and $-\alpha$. Therefore, q quantization levels for quantized SC decoder always have to contain erasure. For this reason, quantization levels for 1-bit decoder with erasure are set to $\{-1, 0, 1\}$ in [23], [24]. As mentioned above, it seems to be essential to include erasure in the quantization levels but in fact it is not. For example, symmetric quantization levels without erasure is used for quantized SC decoder [26]. In Section V, it is explained that the effect of erasure on error-correction performance depends on the number of quantization levels and the channel environment. The simulation results in Section V confirm that if the number of quantization levels and SNR increase, the effect of erasure on error-correction performance decreases because the amount of ambiguity in determining output message at the repetition node is reduced.

IV. NEW NONUNIFORM QUANTIZATION METHODS, CODE CONSTRUCTION STRATEGY, AND QUANTIZED SC DECODER

In this section, based on UB of the BEP and the code construction strategy in [30], new UB expressions including QB values are derived. NQMs and code construction strategy to minimize these UBs are proposed. Finally, a quantized SC decoding scheme based on this NQMs is proposed.

A. UPPER BOUND OF THE BLOCK ERROR PROBABILITY AND CODE CONSTRUCTION STRATEGY

An UB of the BEP $P(E)$ and the code construction strategy for polar codes with SC decoding are explained as given in [30]. Let $B_{i,N}$ be the event that the first error occurs at the ith bit among N bits and $F_{i,N}$ be the event that an error occurs at the ith bit among N bits. The inclusion relation between $B_{i,N}$ and $F_{i,N}$ is given as

$$\begin{aligned} B_{i,N} &= \{u_0^{N-1}, y_0^{N-1} \mid \hat{u}_0^{i-1} = u_0^{i-1}, \hat{u}_i \neq u_i\} \\ &\subseteq \{u_0^{N-1}, y_0^{N-1} \mid \hat{u}_i \neq u_i\} \triangleq F_{i,N}. \end{aligned} \tag{13}$$

The block error event can be expressed as a union of mutually-exclusive events $\{B_{i,N}\}$ over the information set, and by the inclusion relation (13), the BEP $P(E)$ is upper bounded as

$$P(E) = \sum_{i \in \mathcal{I}} P(B_{i,N}) \leq \sum_{i \in \mathcal{I}} P(F_{i,N}). \tag{14}$$

In [30], $P(F_{i,N})$ is evaluated by using density evolution and then $\mathcal{I}$ is selected to minimize $\sum_{i \in \mathcal{I}} P(F_{i,N})$ for constructing polar codes.

In Section IV-B, the UB $\sum_{i \in \mathcal{I}} P(F_{i,N})$ of BEP is transformed into a function of QB variables and SNR. Then, an iterative C2F search algorithm that simultaneously determines QB values and the information set $\mathcal{I}$ by minimizing the objective function, i.e., the UB of BEP, is proposed for the case of $Q = q$. In Section IV-C, NQM and code construction strategy for the case of $Q < q$ are proposed. Based on the QB values and the information set obtained in Section IV-B and IV-C, an NQSC decoding algorithm is proposed in Section IV-D.

B. NONUNIFORM QUANTIZATION METHODS AND CODE CONSTRUCTION STRATEGY FOR THE CASE OF Q=q

1) SYMMETRIC ODD NONUNIFORM QUANTIZATION

Suppose that Q is an odd number and $\vec{a}_M$ denotes $(\underbrace{a, a, a, \cdots, a, a}_{M})$. If channel and decoding algorithm satisfy the symmetry conditions, it is possible to assume that all-zero codeword is transmitted when performing density evolution analysis [29]. So, we assume that a BPSK-modulated vector $\mathbf{v} = \vec{1}_N$ corresponding to the all-zero codeword $\mathbf{x} = \vec{0}_N$ is transmitted because channel symmetry, check node symmetry, and repetition node symmetry are satisfied under the condition of symmetric odd quantization. Let $r_{-\lfloor Q/2 \rfloor + 1}, \cdots, r_{-1}, r_{-0}, r_{+0}, r_1, \cdots, r_{\lfloor Q/2 \rfloor - 1}$ be real

boundary values satisfying $r_{-\lfloor Q/2\rfloor+1} < \cdots < r_{-1} < r_{-0} < r_{+0} < r_1 < \cdots < r_{\lfloor Q/2\rfloor-1}$. Note that $r_{-k} = -r_k$ for $k = +0, 1, 2, \cdots, \lfloor Q/2\rfloor - 1$ due to the symmetry of odd quantization levels resulting from the fact that distributions of $y_i = 1 + n_i$ and $y_i = -1 + n_i$ are symmetric around 0.

To derive a symmetric odd NQM, we perform density evolution analysis. Let m_q be a message symbol of q-level quantized SC decoder. Since $\mathcal{M}_q = \mathcal{M}_Q$, m_q is also an element of $\mathcal{M}_Q$. The SC decoder of polar codes with block length $N = 2^n$ has $n + 1$ stages and there are 2^s node groups at each stage s, e.g., there are 4 stages and 1, 2, 4, 8 node groups at $s = 0, 1, 2, 3$ if $N = 8$ as shown in Fig. 1. By performing density evolution from $s = 1$ to $s = n$, the probabilities of q message symbols corresponding to 2^s node groups at each stage s are updated. Since message symbols of the nodes belonging to the same node group at each stage have the same densities due to the structure of SC decoder, density evolution is performed 2^s times at each stage s. Let $p^{(i)}_{m_q,s}$ be the probability that a message symbol of the ith node group at the stage s is m_q where $0 \le i \le 2^s - 1$. When $s = 0$, $p^{(0)}_{m_q,0} = p_{m_Q}(\gamma)$ where $p_{m_Q}(\gamma)$ denotes the transition probability $\Pr\{f_Q(y_i) = m_Q | v_i = 1\}$ when SNR is γ and $m_Q \in \{-\lfloor Q/2\rfloor, \cdots, -1, 0, 1, \cdots, \lfloor Q/2\rfloor\}$. Through the density evolution from $s = 1$ to $s = n$, $p^{(i)}_{m_q,s}$ can be recursively calculated as follows.

$$\begin{aligned} p^{(2i)}_{\omega,s} &= \sum_{(\mu,\nu)\in S_{\omega,\mathrm{ch}}} p^{(i)}_{\mu,s-1} p^{(i)}_{\nu,s-1} \\ p^{(2i+1)}_{\omega,s} &= \sum_{(\mu,\nu)\in S_{\omega,\mathrm{re}}} p^{(i)}_{\mu,s-1} p^{(i)}_{\nu,s-1} \\ & s = 1, 2, \cdots, n, \;\; i = 0, 1, \cdots, 2^{s-1} - 1 \end{aligned} \tag{15}$$

where

$$\begin{aligned} S_{\omega,\mathrm{ch}} &= \{(\mu, \nu) \,|\, \mu \circ \nu = \omega, \;\; \omega, \mu, \nu \in \mathcal{M}_q\} \\ S_{\omega,\mathrm{re}} &= \{(\mu, \nu) \,|\, \mu \star \nu = \omega, \;\; \omega, \mu, \nu \in \mathcal{M}_q\}. \end{aligned}$$

Example 1 (Density evolution for 5-level quantization): In this example, we will perform density evolution for 5-level quantization. Assume that $\mathcal{M}_Q = \mathcal{M}_q = \{-2, -1, 0, 1, 2\}$. Then, if y_i is in the interval $(-\infty, -r_1)$, $[-r_1, -r_{+0})$, $[-r_{+0}, r_{+0}]$, $(r_{+0}, r_1]$ or (r_1, ∞), the quantizer output m_Q takes the value $-2, -1, 0, 1$ or 2, respectively. According to the message update rules in Section III-C, $S_{\omega,\mathrm{ch}}$ and $S_{\omega,\mathrm{re}}$ are obtained as

$$\begin{aligned} S_{2,\mathrm{ch}} &= \{(2, 2), (-2, -2)\} \\ S_{1,\mathrm{ch}} &= \{(2, 1), (1, 2), (1, 1), (-1, -1), \\ &\quad (-1, -2), (-2, -1)\} \\ S_{0,\mathrm{ch}} &= \{(2, 0), (1, 0), (0, 2), (0, 1), (0, 0), \\ &\quad (0, -1), (0, -2), (-1, 0), (-2, 0)\} \\ S_{-1,\mathrm{ch}} &= \{(2, -1), (1, -1), (1, -2), (-1, 2), \\ &\quad (-1, 1), (-2, 1)\} \\ S_{-2,\mathrm{ch}} &= \{(2, -2), (-2, 2)\} \end{aligned}$$

and

$$\begin{aligned} S_{2,\mathrm{re}} &= \{(2, 2), (2, 1), (2, 0), (1, 2), (0, 2)\} \\ S_{1,\mathrm{re}} &= \{(2, -1), (1, 1), (1, 0), (0, 1), (-1, 2)\} \\ S_{0,\mathrm{re}} &= \{(2, -2), (1, -1), (0, 0), (-1, 1), (-2, 2)\} \\ S_{-1,\mathrm{re}} &= \{(1, -2), (0, -1), (-1, 0), (-1, -1), (-2, 1)\} \\ S_{-2,\mathrm{re}} &= \{(0, -2), (-1, -2), (-2, 0), (-2, -1), (-2, -2)\}. \end{aligned}$$

By using the density evolution equations in (15), $p^{(i)}_{m_q,s}$ can be recursively calculated from $s = 1$ to $s = n$ and the transition probabilities $p_{-2}(\gamma)$, $p_{-1}(\gamma)$, $p_0(\gamma)$, $p_1(\gamma)$, and $p_2(\gamma)$ are calculated as $1 - \mathcal{Q}\left(\frac{-r_1-1}{\sigma}\right)$, $\mathcal{Q}\left(\frac{-r_1-1}{\sigma}\right) - \mathcal{Q}\left(\frac{-r_{+0}-1}{\sigma}\right)$, $\mathcal{Q}\left(\frac{-r_{+0}-1}{\sigma}\right) - \mathcal{Q}\left(\frac{r_{+0}-1}{\sigma}\right)$, $\mathcal{Q}\left(\frac{r_{+0}-1}{\sigma}\right) - \mathcal{Q}\left(\frac{r_1-1}{\sigma}\right)$, and $\mathcal{Q}\left(\frac{r_1-1}{\sigma}\right)$, respectively, where $\mathcal{Q}(x) = \frac{1}{\sqrt{2\pi}} \int_x^\infty e^{-\frac{t^2}{2}} dt$.

Next, the error probability of each bit of polar code is calculated by density evolution equations in (15), and UB of the BEP is calculated by using these bit error probabilities where UB is a function of QB variables and SNR. Then, polar codes are constructed by simultaneously determining the information set $\mathcal{I}$ and the QB values that minimize the UB. Let $p^{(i)}_N = \Pr\{\hat{u}_i \ne 0 | u_i = 0\}$ be the probability that an error occurs at the ith transmitted bit among N bits when all-zero codeword is transmitted. In the quantized SC decoding, u_i is estimated, $0 \le i \le N - 1$, such that $\hat{u}_i$ is 0 if the ith decoded message symbol m_q is larger than 0 and $\hat{u}_i$ is 1 if the ith decoded message symbol m_q is smaller than 0, i.e., $\{1, 2, \cdots, \lfloor Q/2\rfloor\} \to 0$ and $\{-1, -2, \cdots, -\lfloor Q/2\rfloor\} \to 1$. Especially, $\hat{u}_i$ is determined by choosing 0 or 1 uniformly at random if the ith decoded message symbol m_q is 0. Then, $p^{(i)}_N$ can be expressed as a summation of $p^{(i)}_{m_q,n}$'s for $m_q = 0, -1, -2, \cdots, -\lfloor Q/2\rfloor$, where each $p^{(i)}_{m_q,n}$ is a function of QB values and SNR γ for the Q-level quantizer. Let $\mathbf{r}'_Q$ and $\mathbf{r}_Q$ be the sets of QB values $\{r_{-\lfloor Q/2\rfloor+1}, \cdots, r_{-0}, r_{+0}, \cdots, r_{\lfloor Q/2\rfloor-1}\}$ and $\{r_{+0}, r_1, \cdots, r_{\lfloor Q/2\rfloor-1}\}$, respectively, and $F_{i,N,\mathbf{x}}(\mathbf{r}_Q, \gamma)$ denotes the event that an error occurs at the ith bit among N bits when a codeword $\mathbf{x}$ is transmitted, QB values are $\mathbf{r}_Q$, and SNR is γ. Then, $p^{(i)}_N$, $0 \le i \le N - 1$, can be written as

$$\begin{aligned} p^{(i)}_N &= \frac{1}{2} p^{(i)}_{0,n} + \sum_{j=-1}^{-\lfloor Q/2\rfloor} p^{(i)}_{j,n} \\ &\triangleq P\big(F_{i,N,\vec{0}_N}(\mathbf{r}'_Q, \gamma)\big) = P\big(F_{i,N,\vec{0}_N}(\mathbf{r}_Q, \gamma)\big) \end{aligned} \tag{16}$$

where it is assumed that all-zero codeword $\vec{0}_N$ is transmitted. Then, QBs for Q-level quantizer and the information set $\mathcal{I}$ over AWGN channel are simultaneously determined by solving

$$\begin{aligned} &\hat{r}_{+0}, \hat{r}_1, \cdots, \hat{r}_{\lfloor Q/2\rfloor-1}, \mathcal{I} \\ &= \arg \min_{\substack{0<r_{+0}<r_1<\cdots<r_{\lfloor Q/2\rfloor-1}\in\mathbb{R} \\ \mathcal{I}\subseteq[N],\ |\mathcal{I}|=NR}} \sum_{i\in\mathcal{I}} P\big(F_{i,N,\vec{0}_N}(\mathbf{r}_Q, \gamma)\big) \end{aligned} \tag{17}$$

where $[N] \triangleq \{0, 1, \cdots, N - 1\}$ and $\sum_{i\in\mathcal{I}} P\big(F_{i,N,\vec{0}_N}(\mathbf{r}_Q, \gamma)\big)$ denotes the UB of BEP in (14) when all-zero codeword is transmitted, QB values are $\mathbf{r}_Q$, and SNR is γ.

2) THE PROPOSED ITERATIVE COARSE-TO-FINE (C2F) SEARCH ALGORITHM FOR SOLVING THE MINIMIZATION PROBLEM

Since the UB of BEP in (17) is a recursive function of QB variables and SNR obtained by using density evolution as explained in Section IV-B1, the solution of the minimization problem in (17) cannot be analytically calculated. Therefore, some search algorithms to determine QB values and the information set $\mathcal{I}$ are proposed in Algorithms 4-6.

Algorithm 4 is an exhaustive search algorithm, which is a trivial deterministic search algorithm to solve the minimization problem. In Algorithm 4, Sort($\mathbf{s}$) is a function that outputs two sets $\mathbf{s}_{\text{val}}$ and $\mathbf{s}_{\text{idx}}$ where $\mathbf{s}_{\text{val}}$ and $\mathbf{s}_{\text{idx}}$ denote the rearranged set of $\mathbf{s}$ in ascending order and the set of indices of $\mathbf{s}_{\text{val}}$ in that order, respectively, e.g., when $\mathbf{s} = \{5, 4, 9, 2\}$, $\mathbf{s}_{\text{val}} = \{2, 4, 5, 9\}$ and $\mathbf{s}_{\text{idx}} = \{3, 1, 0, 2\}$. Also, η and $\sum^*$ denote the number of steps and UB of BEP according to η, respectively. Throughout the paper, the resolution of QB value is set as $\tau = 0.0001$. The structure of Algorithm 4 can be interpreted as a tree structure. Denote the number of children of each node and the length of the longest downward path from a root node to a leaf node by the degree of each node and height of a tree structure, respectively. The degree of a tree structure is the maximum degree of a node in the tree structure. Then, Algorithm 4 has the tree structure with the maximum degree c/τ and the height N_r with some constant c, and its computational complexity is $\mathcal{O}((c/\tau)^{N_r})$. This implies that for large Q and small τ, it is impossible to obtain the solution of the minimization problem in (17) by Algorithm 4.

To solve this problem, an iterative C2F algorithm based on the concept of random walk [31] is proposed. Unlike random walk which has a constant travel distance for each step [31], the proposed algorithm applies a varying travel distance for each step. Specifically, the proposed iterative C2F search algorithm probabilistically reduces the objective function by coarsely changing each QB value at first and then gradually changing it finely. The steps of coarsely and finely changing QBs form one loop, and this loop is iterated until a stopping criterion is satisfied. The pseudo code of the proposed iterative C2F search algorithm is presented in Algorithm 5, which minimizes UB of BEP by searching the QB values and the information set $\mathcal{I}$ for symmetric odd nonuniform quantization levels. In Algorithm 5, unif(a, b) denotes the continuous uniform distribution where the support of this distribution is the open interval (a, b) and $v \sim f$ means that a random variable v is sampled from the distribution f. Note that for each loop, β determines the support of the continuous uniform distribution and ϵ controls the size of β to coarsely or finely change QB values. Finally, δ denotes the number of loops during which the objective function is kept at the minimum value, and the iterative C2F search algorithm is finished if $\delta = \delta^*$.

3) ASYMMETRIC EVEN NONUNIFORM QUANTIZATION

For the asymmetric even quantization, the number of positive quantization levels is one more than the number of negative quantization levels, or vice versa, and the former is considered in this paper. Note that there is no difference in error-correction performance in these two cases because the transmitted information bits are selected uniformly at random and so it does not matter whether the former or the latter is considered. Since the quantization levels are asymmetric around erasure ($= 0$) as shown in Fig. 2(b), we cannot assume that only all-zero codeword is transmitted. However, if all possible codewords are considered, analysis becomes too complicated. Therefore, we only consider two extreme cases such that BPSK-modulated vectors $\mathbf{v} = \vec{1}_N$ for all-zero codeword $\mathbf{x} = \vec{0}_N G_N = \vec{0}_N$ and $\mathbf{v} = -\vec{1}_N$ for all-one codeword $\mathbf{x} = (\underbrace{0, 0, 0, \cdots, 0, 1}_{N})G_N = \vec{1}_N$ are transmitted. Based on this consideration, it is proposed that $Q - 2$ QB values $\hat{r}_{-Q/2+2}, \cdots, \hat{r}_{-0}, \hat{r}_{+0}, \cdots, \hat{r}_{Q/2-2}$ are obtained by solving the problem in (17) under the assumption that all-zero codeword is transmitted due to the symmetry of quantization levels and then the remaining boundary value $r_{Q/2-1}$ is determined such that the average of UBs of block error probabilities for these two extreme cases is minimized. Since the number and positions of $1'$s in a BPSK-modulated

Algorithm 4: Exhaustive Search Algorithm of QB Values and the Information Set $\mathcal{I}$ for Symmetric Odd and Even Nonuniform Quantization Levels by Minimizing UB of BEP

Inputs: Q, N, R, γ, τ.
Outputs: $\hat{\mathbf{r}}_Q, \mathcal{I}$.
if Q is odd **then**
  $N_r \leftarrow \lfloor Q/2 \rfloor$, $\{r_Q[0], \cdots, r_Q[N_r - 1]\} \leftarrow \vec{0}_{\lfloor Q/2 \rfloor}$
else if Q is even **then**
  $N_r \leftarrow Q/2 - 1$, $\{r_Q[0], \cdots, r_Q[N_r - 1]\} \leftarrow \vec{0}_{Q/2-1}$
$\sum_{\text{temp}} \leftarrow \infty$, $\sum^* \leftarrow \infty$, $\eta \leftarrow 0$
for $r_Q[0] = \tau : \tau : \infty$ **do**
  for $r_Q[1] = \tau : \tau : \infty$ **do**
    $\cdots$
    for $r_Q[N_r - 1] = \tau : \tau : \infty$ **do**
      if $0 < r_Q[0] < r_Q[1] < \cdots < r_Q[N_r - 1]$ **then**
        /* The starting point of one step */
        Calculate transition probabilities $p_{m_Q}(\gamma)$ for $m_Q \in \mathcal{M}_Q$
        Calculate $P\big(F_{i,N,\vec{0}_N}(\mathbf{r}_Q, \gamma)\big)$ by using (15), (16), and (21) for $i = 0, \cdots, N-1$
        $[\mathbf{s}_{\text{val}}, \mathbf{s}_{\text{idx}}] \leftarrow \text{Sort}\big(\{P\big(F_{i,N,\vec{0}_N}(\mathbf{r}_Q, \gamma)\big)\}_{i=0}^{N-1}\big)$
        $\sum \leftarrow$ the sum of all elements of $\{\mathbf{s}_{\text{val}}[i]\}_{i=0}^{NR-1}$
        if $\sum \le \sum_{\text{temp}}$ **then**
          $\sum_{\text{temp}} \leftarrow \sum$, $\hat{\mathbf{r}}_{Q,\text{temp}} \leftarrow \mathbf{r}_Q$, $\mathcal{I}_{\text{temp}} \leftarrow \{\mathbf{s}_{\text{idx}}[i]\}_{i=0}^{NR-1}$
        else
          if $\sum^* > \sum_{\text{temp}}$ **then**
            $\sum^* \leftarrow \sum_{\text{temp}}$, $\hat{\mathbf{r}}_Q \leftarrow \hat{\mathbf{r}}_{Q,\text{temp}}$, $\mathcal{I} \leftarrow \mathcal{I}_{\text{temp}}$
          $\sum_{\text{temp}} \leftarrow \infty$ and break;
        $\eta \leftarrow \eta + 1$
        /* The end point of one step */

Algorithm 5: Iterative Coarse-to-Fine Search Algorithm of QB Values and the Information Set $\mathcal{I}$ for Symmetric Odd and Even Nonuniform Quantization Levels by Minimizing UB of BEP

Inputs: $Q, N, R, \gamma, \tau, \beta_{\text{ini}}, \epsilon, \delta^*$.
Outputs: $\hat{\mathbf{r}}_Q, \mathcal{I}$.
if Q is odd **then**
  $N_r \leftarrow \lfloor Q/2 \rfloor$
else if Q is even **then**
  $N_r \leftarrow Q/2 - 1$
while (1) **do**
  $\{r_Q[0], \cdots, r_Q[N_r - 1]\} \leftarrow \{v : v \sim \text{unif}(0, \beta_{\text{ini}})\}^{N_r}$
  if $0 < r_Q[0] < \cdots < r_Q[N_r - 1]$ **then**
    break;
$\beta \leftarrow \beta_{\text{ini}}, \sum_{\text{temp}} \leftarrow \infty, \sum^* \leftarrow \infty$
while (1) **do**
  /* The starting point of one step */
  Calculate the transition probabilities $p_{m_Q}(\gamma)$ for $m_Q \in \mathcal{M}_Q$
  Calculate $P\big(F_{i,N,\vec{0}_N}(\mathbf{r}_Q, \gamma)\big)$ by using (15), (16), and (21) for $i = 0, \cdots, N-1$
  $[\mathbf{s}_{\text{val}}, \mathbf{s}_{\text{idx}}] \leftarrow \text{Sort}\big(\{P\big(F_{i,N,\vec{0}_N}(\mathbf{r}_Q, \gamma)\big)\}_{i=0}^{N-1}\big)$
  $\sum \leftarrow$ the sum of all elements of $\{\mathbf{s}_{\text{val}}[i]\}_{i=0}^{NR-1}$
  if $\sum \le \sum_{\text{temp}}$ **then**
    $\sum_{\text{temp}} \leftarrow \sum, \hat{\mathbf{r}}_{Q,\text{temp}} \leftarrow \mathbf{r}_Q, \mathcal{I}_{\text{temp}} \leftarrow \{\mathbf{s}_{\text{idx}}[i]\}_{i=0}^{NR-1}$
  else
    $\mathbf{r}_Q \leftarrow \hat{\mathbf{r}}_{Q,\text{temp}}$
  while (1) **do**
    $\mathbf{r}_{Q,\text{temp}} \leftarrow \mathbf{r}_Q + \{v : v \sim \text{unif}(-\beta, \beta)\}^{N_r}$
    if $0 < r_{Q,\text{temp}}[0] < \cdots < r_{Q,\text{temp}}[N_r - 1]$ **then**
      break;
  $\mathbf{r}_Q \leftarrow \mathbf{r}_{Q,\text{temp}}$
  if $\epsilon \cdot \beta \ge \tau$ **then**
    $\beta \leftarrow \epsilon \cdot \beta$
  else
    $\beta \leftarrow \beta_{\text{ini}}$
    if $\sum^* > \sum_{\text{temp}}$ **then**
      $\sum^* \leftarrow \sum_{\text{temp}}, \delta \leftarrow 0$
    else if $\sum^* = \sum_{\text{temp}}$ **then**
      $\delta \leftarrow \delta + 1$
  if $\delta = \delta^*$ **then**
    $\hat{\mathbf{r}}_Q \leftarrow \hat{\mathbf{r}}_{Q,\text{temp}}, \mathcal{I} \leftarrow \mathcal{I}_{\text{temp}}$, and break;
  /* The end point of one step */

vector $\mathbf{v}$ affect the determination of the QB value $r_{Q/2-1}$, e.g., $r_{Q/2-1} \to \hat{r}_{Q/2-2}$ if $\mathbf{v} = \vec{1}_N$ and $r_{Q/2-1} \to \infty$ if $\mathbf{v} = -\vec{1}_N$, we consider these two extreme cases with the largest number of 1′s and the smallest number of 1′s. Also, due to the all-one codeword, 1′s complement of any codeword is also a codeword, which justifies our approach.

The message alphabet $\mathcal{M}_Q$ for asymmetric even nonunifrom quantizer is given as $\{-Q/2+1, \cdots, -1, 0, 1, \cdots, Q/2\}$. Let $\hat{\mathbf{r}}_{Q-2} = \{\hat{r}_{-Q/2+2}, \cdots, \hat{r}_{-1}, \hat{r}_{-0}, \hat{r}_{+0}, \hat{r}_1, \cdots, \hat{r}_{Q/2-2}\}$ be $Q-2$ symmetric QB values obtained from (17) and $r_{Q/2-1}$ be a real number satisfying $r_{Q/2-1} > r_{Q/2-2}$. Since $\mathcal{M}_Q = \mathcal{M}_q$, the message symbol m_q for SC decoding is also an element of $\mathcal{M}_Q$. Similar to the proposed symmetric odd NQM, for the above-mentioned two extreme cases, the probability $p_{m_q,s}^{(i)}$ of a message symbol of the ith node being m_q at the stage s can be obtained through density evolution analysis by using the recursive equations in (15). For the all-zero codeword, $p_{m_q,0}^{(i)}$ in (15) denotes the transition probability $\Pr\{f_Q(y_i) = m_Q | v_i = 1\}$ and for the all-one codeword, $p_{m_q,0}^{(i)}$ in (15) denotes the transition probability $\Pr\{f_Q(y_i) = m_Q | v_i = -1\}$.

When all-zero codeword is transmitted, i.e., $\mathbf{u} = \vec{0}_N$, $p_N^{(i)}$, $0 \le i \le N-1$, can be expressed as

$$p_N^{(i)} = \Pr\{\hat{u}_i \neq 0 | u_i = 0\} = \frac{1}{2} p_{0,n}^{(i)} + \sum_{j=-1}^{-Q/2+1} p_{j,n}^{(i)} \triangleq P\big(F_{i,N,\vec{0}_N}(\hat{\mathbf{r}}_{Q-2}, r_{Q/2-1}, \gamma)\big). \tag{18}$$

When all-one codeword is transmitted, i.e., $\mathbf{u} = \{\underbrace{0, 0, 0, \cdots, 0, 1}_{N}\}$, $p_N^{(i)}$, $0 \le i \le N-1$, can be expressed as

$$p_N^{(i)} = \begin{cases} \Pr\{\hat{u}_i \neq 0 | u_i = 0\} \\ = \frac{1}{2} p_{0,n}^{(i)} + \sum_{j=-1}^{-Q/2+1} p_{j,n}^{(i)}, & \text{if } 0 \le i \le N-2 \\ \Pr\{\hat{u}_i \neq 1 | u_i = 1\} \\ = \frac{1}{2} p_{0,n}^{(i)} + \sum_{j=1}^{Q/2} p_{j,n}^{(i)}, & \text{if } i = N-1 \end{cases} \triangleq P\big(F_{i,N,\vec{1}_N}(\hat{\mathbf{r}}_{Q-2}, r_{Q/2-1}, \gamma)\big). \tag{19}$$

Then, after the QBs $\hat{\mathbf{r}}_{Q-2}$ are obtained by (17), the remaining $r_{Q/2-1}$ and the information set $\mathcal{I}$ over AWGN channel are determined by solving

$$\hat{r}_{Q/2-1}, \mathcal{I} = \arg \min_{\hat{r}_{Q/2-2} < r_{Q/2-1} \in \mathbb{R} \mathcal{I} \subseteq [N],\ |\mathcal{I}| = NR} \times \frac{1}{2} \sum_{i \in \mathcal{I}} \Big\{ P\big(F_{i,N,\vec{0}_N}(\hat{\mathbf{r}}_{Q-2}, r_{Q/2-1}, \gamma)\big) + P\big(F_{i,N,\vec{1}_N}(\hat{\mathbf{r}}_{Q-2}, r_{Q/2-1}, \gamma)\big) \Big\}. \tag{20}$$

The pseudo code of the exhaustive search algorithm is presented in Algorithm 6, which minimizes UB of BEP by searching the QB value $\hat{r}_{Q/2-1}$ and the information set $\mathcal{I}$ for asymmetric even nonuniform quantization levels.

4) SYMMETRIC EVEN NONUNIFORM QUANTIZATION

A symmetric even NQM is almost similar to the symmetric odd NQM explained in Section IV-B1. We assume that all-zero codeword $\mathbf{x} = \vec{0}_N$ is transmitted. Let $r_{-Q/2+1}, \cdots, r_{-1}, 0, r_1, \cdots, r_{Q/2-1}$ be the QB values satisfying $r_{-Q/2+1} < \cdots < r_{-1} < 0 < r_1 < \cdots < r_{Q/2-1}$. Note that $r_{-k} = -r_k$ for $k = 1, 2, \cdots, Q/2-1$. Through the density evolution from $s = 1$ to $s = n$, $p_{m_q,s}^{(i)}$'s are calculated from (15) by replacing the operation $\star$ in (15) by the operation $*$. The ith bit error probability

Algorithm 6: Exhaustive Search Algorithm of a QB Value $\hat{r}_{Q/2-1}$ and the Information Set $\mathcal{I}$ for Asymmetric Even Nonuniform Quantization Levels by Minimizing UB of BEP

Inputs: $Q, N, R, \gamma, \hat{\mathbf{r}}_{Q-2}, \tau$.
Outputs: $\hat{r}_{Q/2-1}, \mathcal{I}$.
$\sum^* \leftarrow \infty$
for $r_{Q/2-1} = \hat{r}_{Q/2-2} + \tau : \tau : \infty$ **do**
  Calculate the transition probabilities $p_{m_Q}(\gamma)$ for $m_Q \in \mathcal{M}_Q$
  Calculate $P\big(F_{i,N,\vec{0}_N}(\hat{\mathbf{r}}_{Q-2}, r_{Q/2-1}, \gamma)\big)$ by using (15) and (18), and calculate $P\big(F_{i,N,\vec{1}_N}(\hat{\mathbf{r}}_{Q-2}, r_{Q/2-1}, \gamma)\big)$ by using (15) and (19) for $i = 0, \cdots, N-1$
  $[\mathbf{s}_{\text{val}}, \mathbf{s}_{\text{idx}}] \leftarrow \text{Sort}\Big(\frac{1}{2}\Big\{P\big(F_{i,N,\vec{0}_N}(\hat{\mathbf{r}}_{Q-2}, r_{Q/2-1}, \gamma)\big) + P\big(F_{i,N,\vec{1}_N}(\hat{\mathbf{r}}_{Q-2}, r_{Q/2-1}, \gamma)\big)\Big\}_{i=0}^{N-1}\Big)$
  $\sum \leftarrow$ the sum of all elements of $\{\mathbf{s}_{\text{val}}[i]\}_{i=0}^{NR-1}$
  if $\sum \le \sum^*$ **then**
    $\sum^* \leftarrow \sum, \hat{r}_{Q/2-1} \leftarrow r_{Q/2-1}, \mathcal{I} \leftarrow \{\mathbf{s}_{\text{idx}}[i]\}_{i=0}^{NR-1}$
  else
    break;

$p_N^{(i)}, 0 \le i \le N-1$, can be expressed as

$$p_N^{(i)} = \sum_{j=-1}^{-Q/2} p_{j,n}^{(i)} \triangleq P\big(F_{i,N,\vec{0}_N}(\mathbf{r}'_Q, \gamma)\big) = P\big(F_{i,N,\vec{0}_N}(\mathbf{r}_Q, \gamma)\big) \tag{21}$$

where $\mathbf{r}'_Q$ and $\mathbf{r}_Q$ are $\{r_{-Q/2+1}, \cdots, r_{-1}, 0, r_1, \cdots, r_{Q/2-1}\}$ and $\{r_1, \cdots, r_{Q/2-1}\}$, respectively. Then, QBs and the information set $\mathcal{I}$ over AWGN channel are determined by solving

$$\hat{r}_1, \hat{r}_2, \cdots, \hat{r}_{Q/2-1}, \mathcal{I} = \arg \min_{\substack{0<r_1<r_2<\cdots<r_{Q/2-1}\in\mathbb{R} \\ \mathcal{I}\subseteq[N], |\mathcal{I}|=NR}} \sum_{i\in\mathcal{I}} P\big(F_{i,N,\vec{0}_N}(\mathbf{r}_Q, \gamma)\big). \tag{22}$$

The pseudo code of the proposed iterative C2F search algorithm is presented in Algorithm 5, which minimizes UB of BEP by searching the QB values and the information set $\mathcal{I}$ for symmetric even nonuniform quantization levels.

C. NONUNIFORM QUANTIZATION METHOD AND CODE CONSTRUCTION STRATEGY USING A SCALING METHOD FOR THE CASE OF Q<q

So far, quantization methods are derived under the assumption that $Q = q$. In this section, we propose a NQM for the case of $Q < q$. The output message values of check and repetition node operations for 2 input messages (m_0, m_1) are smaller than or equal to $\max(m_0, m_1)$ and larger than or equal to $\min(m_0, m_1)$. To match the largest and smallest elements of $\mathcal{M}_Q$ to those of $\mathcal{M}_q$, a scaling factor is utilized in quantized SC decoder. In this section, we will propose a symmetric even NQM with the scaling factor for ease of explanation and this approach can be easily applied to derive symmetric odd quantization method and asymmetric even quantization method.

In the symmetric even NQM, $\mathcal{M}_Q = \{-Q/2, \cdots, -1, 1, \cdots, Q/2\}$ and $\mathcal{M}_q = \{-q/2, \cdots, -1, 1, \cdots, q/2\}$ where Q and q are even numbers with $Q < q$. The received value y_i is quantized to a message symbol $m_Q \in \mathcal{M}_Q$ by using the quantization function (10). Let $m_Q^{\max}, m_Q^{\min} \in \mathcal{M}_Q$ and $m_q^{\max}, m_q^{\min} \in \mathcal{M}_q$ be the largest and smallest elements of $\mathcal{M}_Q$ and $\mathcal{M}_q$, respectively. To adjust the output values m_Q of quantizer suitable for the message values m_q of quantized SC decoder, m_Q is scaled as $m_Q^+ = \lfloor \lambda_+ \cdot m_Q \rfloor$ if $m_Q \ge 0$ or $m_Q^- = \lceil \lambda_- \cdot m_Q \rceil$ if $m_Q < 0$. Here, λ_+ and λ_- are the scaling factors defined as $\lambda_+ = m_q^{\max}/m_Q^{\max}$ and $\lambda_- = m_q^{\min}/m_Q^{\min}$. Also, $\mathcal{M}_Q^{(\text{new})}$ is a new message alphabet consisting of the scaled messages m_Q^+ and m_Q^- for NQSC decoder.

Example 2 (Scaled message symbols of nonuniform quantizer when $Q = 4$ and $q = 8$:) For $\mathcal{M}_Q = \{-2, -1, 1, 2\}$ and $\mathcal{M}_q = \{-4, -3, -2, -1, 1, 2, 3, 4\}$, $\mathcal{M}_Q^{(\text{new})}$ is obtained as $\{-4, -2, 2, 4\}$ by scaling $\mathcal{M}_Q$ with the scaling factors $\lambda_+ = \lambda_- = 2$. Therefore, a received value y_i in the interval $(-\infty, -r_1), [-r_1, 0), [0, r_1]$ or (r_1, ∞) is quantized into $-2, -1, 1$, or 2 by quantizer and then scaled into $-4, -2, 2, 4$, respectively.

For the case of $Q < q$, NQM and code construction strategy are the same as those of the proposed NQMs for $Q = q$.

D. NONUNIFROM-QUANTIZED SC DECODING ALGORITHM

Let $m_q^{(s)}(\phi, \omega) \in \mathcal{M}_q$ be the message symbol and $b^{(s)}(\phi, \omega)$ be the bit-decision (0 or 1) of the node ω in the node group ϕ at the stage s in the quantized SC decoder as explained in Section II-D. Hereafter, the bit-decision $b^{(s)}(\phi, \omega)$ is represented in the message form rather than 0 or 1, i.e., 0 and 1 are represented by $m_q^{\max}$ and $m_q^{\min}$, respectively, and if there is no information before being determined, the bit-decision is expressed as 0. At the quantizer, each received value y_i of a received vector $\mathbf{y} = y_0^{N-1}$ is mapped to a quantized message symbol m_Q by using the quantization functions (8), (9), and (10) based on the QB values obtained by solving (17), (20), and (22), i.e., $f_Q(y_i) = m_Q \in \mathcal{M}_Q$. Then, the quantized message symbols of the quantizer $f_Q(y_i)$ are scaled to the input message symbols of quantized SC decoder $m_q^{(0)}(0, i)$ as

$$m_q^{(0)}(0, i) = \begin{cases} f_Q(y_i), & \text{if } Q = q \\ \lfloor \lambda_+ \cdot f_Q(y_i) \rfloor, & \text{if } Q < q \text{ and } f_Q(y_i) \ge 0 \\ \lceil \lambda_- \cdot f_Q(y_i) \rceil, & \text{if } Q < q \text{ and } f_Q(y_i) < 0. \end{cases} \tag{23}$$

With the zero-fixed frozen bits $\mathbf{u}_{\mathcal{I}^c}$, the information set $\mathcal{I}$, and the input messages $\{m_q^{(0)}(0, i)\}_{i=0}^{N-1}$, the bit-decisions $\{b^{(n)}(i, 0)\}_{i=0}^{N-1}$ are calculated in the quantized SC decoder. By using these bit-decisions $\{b^{(n)}(i, 0)\}_{i=0}^{N-1}$, the message bits $u_0^{N-1}, i = 0, 1, \cdots, N-1$, are estimated as

$$\hat{u}_i \triangleq \begin{cases} 0, & \text{if } i \in \mathcal{I}^c \text{ or } b^{(n)}(i, 0) > 0 \\ 1, & \text{otherwise.} \end{cases} \tag{24}$$

Note that $\mathcal{I}$ is obtained by (17) or (20). For initialization of quantized SC decoding, the input message symbols $m_q^{(0)}(0,i)$ are set by (23) and the bit-decisions $b^{(0)}(0,i)$, $i=0,1,\ldots,N-1$, are initialized as

$$b^{(0)}(0,i)=\begin{cases} m_q^{\max}, & \text{if } i\in\mathcal{I}^c \\ 0, & \text{otherwise} \end{cases} \tag{25}$$

where the bit-decisions $b^{(0)}(0,i)$ initialized to 0 for $i\in\mathcal{I}$ indicate that there is no information about $\mathbf{u}_{\mathcal{I}}$ in the initialization stage of quantized SC decoding as explained in Section II-D. For $i=0,1,\cdots,N-1$, $m_q^{(n)}(i,0)$ is sequentially calculated by the recursion

$$m_q^{(s)}(\phi,\omega)=m_q^{(s-1)}(\psi,2\omega)\circ m_q^{(s-1)}(\psi,2\omega+1) \tag{26}$$

for even ϕ, and

$$m_q^{(s)}(\phi,\omega)=m_q^{(s-1)}(\psi,2\omega+1) \star\big(m_q^{(s-1)}(\psi,2\omega)\circ b^{(s)}(\phi-1,\omega)\big) \tag{27}$$

for odd ϕ where $\psi=\lfloor\frac{\phi}{2}\rfloor$. Note that for symmetric even quantized SC decoding without erasure, the operation $*$ defined in (12) is used instead of the operation $\star$ in (27). Whenever $m_q^{(n)}(i,0)$ is calculated for each $i\in\mathcal{I}$, $b^{(n)}(i,0)$ is updated by

$$b^{(n)}(i,0)=\begin{cases} m_q^{\max}, & \text{if } m_q^{(n)}(i,0)>0 \\ m_q^{\max} \text{ or } m_q^{\min}, & \text{if } m_q^{(n)}(i,0)=0 \\ m_q^{\min}, & \text{otherwise} \end{cases} \tag{28}$$

where $\Pr\big(b^{(n)}(i,0)=m_q^{\max}|m_q^{(n)}(i,0)=0\big)=\Pr\big(b^{(n)}(i,0)=m_q^{\min}|m_q^{(n)}(i,0)=0\big)=1/2$. Also, whenever $m_q^{(n)}(i,0)$ is updated for odd value of ϕ, $b^{(s)}(\phi,\omega)$ is updated by

$$\begin{aligned} b^{(s-1)}(\psi,2\omega)&=b^{(s)}(\phi-1,\omega)\circ b^{(s)}(\phi,\omega) \\ b^{(s-1)}(\psi,2\omega+1)&=b^{(s)}(\phi,\omega) \end{aligned} \tag{29}$$

where $\psi=\lfloor\frac{\phi}{2}\rfloor$. The pseudo code of NQSC decoding algorithm is presented as Algorithms 7-9. Algorithm 7 is the main algorithm of NQSC decoding, and bit-decision and message symbol at each node are updated as in Algorithms 8 and 9, respectively. Note that for the symmetric even quantized SC decoding, the operation $*$ in Algorithm 9 is replaced by the operation $\star$.

V. SIMULATION RESULTS

For the block length $N=1024$, the code rate $R=0.5$, and $Q=q\in\{3,4\}$, UBs and simulated BEPs of the proposed NQSC decoding over AWGN channel are compared in Fig. 4. Note that the UB of BEP for symmetric odd NQSC decoding is obtained by (17) and the UBs of BEP for asymmetric and symmetric even NQSC decodings are obtained by (20) and (22), respectively. To avoid the case that UB is larger than 1, the UB is determined as min{1, calculated UB}. Also, the simulated block error probabilities of NQSC decoding for $Q=4$ and $q=8,16,32$ are shown in Fig. 4. For $Q=q=4$ (2-bit precision quantization), it is confirmed that the proposed asymmetric and symmetric NQSC decoders show 2.9dB and 2.5dB better performance at the BEP 10^{-4} compared to the optimal uniform-quantized SC decoder [26],

Algorithm 7: Nonuniform-Quantized SC Decoding

$\{y_i\}_{i=0}^{N-1}\leftarrow$ the received values from channel
$\{f_Q(y_i)\}_{i=0}^{N-1}\leftarrow$ the output values of the quantizer
$\{m_q^{(0)}(0,i)\}_{i=0}^{N-1}\leftarrow$ the input message values of the quantized SC decoder
$\{b^{(n)}(i,0)\}_{i\in\mathcal{I}^c}\leftarrow m_q^{\max}$, $\{b^{(n)}(i,0)\}_{i\in\mathcal{I}}\leftarrow 0$
for $\phi=0\rightarrow N-1$ **do**
  UpdateQuantizedMessageMap(n,ϕ)
  if $\phi\in\mathcal{I}$ **then**
    if $m_q^{(n)}(\phi,0)>0$ **then**
      $b^{(n)}(\phi,0)\leftarrow m_q^{\max}$
    else if $m_q^{(n)}(\phi,0)=0$ **then**
      $b^{(n)}(\phi,0)\leftarrow m_q^{\max}$ or $m_q^{\min}$ with probability $1/2$
    else
      $b^{(n)}(\phi,0)\leftarrow m_q^{\min}$
  if ϕ is odd **then**
    UpdateQuantizedBitMap(n,ϕ)
for $i=0\rightarrow N-1$ **do**
  if $i\in\mathcal{I}^c$ or $b^{(n)}(i,0)>0$ **then**
    $\hat{u}_i\leftarrow 0$
  else
    $\hat{u}_i\leftarrow 1$

Algorithm 8: UpdateQuantizedBitMap(s,ϕ)

if ϕ is odd **then**
  for $\omega=0\rightarrow 2^{n-s}-1$ **do**
    $b^{(s-1)}(\psi,2\omega)\leftarrow b^{(s)}(\phi-1,\omega)\circ b^{(s)}(\phi,\omega)$
    $b^{(s-1)}(\psi,2\omega+1)\leftarrow b^{(s)}(\phi,\omega)$
  if ψ is odd **then**
    UpdateQuantizedBitMap$(s-1,\psi)$

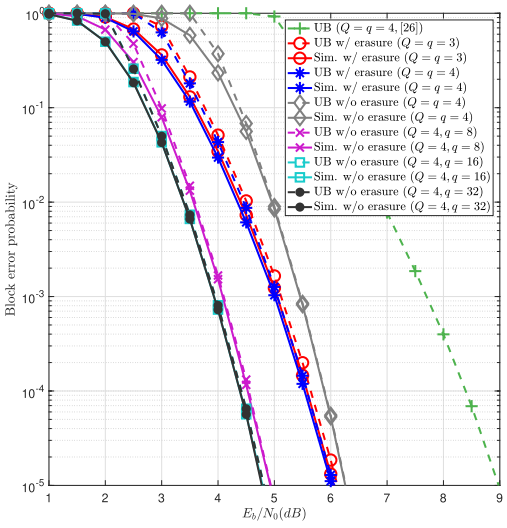

FIGURE 4. UBs and simulated BEPs of uniform-quantized SC decoding [26] and NQSC decoding for $Q=q\in\{3,4\}$, and $Q=4$ and $q=8,16,32$ over AWGN channel ($N=1024$, $R=0.5$).

Algorithm 9: UpdateQuantizedMessageMap(s, ϕ)

if $s = 0$ **then**
  return $\psi \leftarrow \lfloor \frac{\phi}{2} \rfloor$
if ϕ is even **then**
  UpdateQuantizedMessageMap($s-1, \psi$)
for $\omega = 0 \rightarrow 2^{n-s} - 1$ **do**
  if ϕ is even **then**
    $m_q^{(s)}(\phi, \omega) \leftarrow m_q^{(s-1)}(\psi, 2\omega) \circ m_q^{(s-1)}(\psi, 2\omega+1)$
  else
    $m_q^{(s)}(\phi, \omega)$
    $\leftarrow m_q^{(s-1)}(\psi, 2\omega+1) \star \left(m_q^{(s-1)}(\psi, 2\omega) \circ b^{(s)}(\phi-1, \omega)\right)$

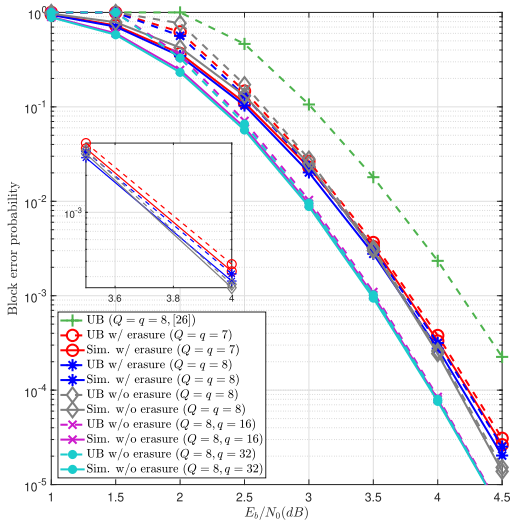

FIGURE 5. UBs and simulated BEPs of uniform-quantized SC decoding [26] and NQSC decoding for $Q = q \in \{7, 8\}$, and $Q = 8$ and $q = 16, 32$ over AWGN channel ($N = 1024$, $R = 0.5$).

respectively. Since UBs and block error probabilities of [26] are almost the same according to SNR, in this paper, the error correcting performance of the proposed method is compared to the UB of BEP of optimal uniform-quantized SC decoding [26]. Although asymmetric 4-level NQSC decoder with erasure is better than symmetric 4-level NQSC decoder without erasure for SNR below 6.5dB, these two BEP curves will be crossed at some SNR higher than 6.5dB. This means that the effect of erasure decreases as SNR increases. Also, Fig. 4 shows that NQSC decoder for $Q = 4$ and $q = 8, 16, 32$ outperforms the NQSC decoder for $Q = q = 4$ for all SNR range. This means that without raising the number of quantization levels for quantizer, the block error-correction performance can be improved by increasing the number of quantization levels for quantized SC decoder. However, the amount of improvement decreases as q increases and no longer improves after some q value (say, $q > 16$ in Fig. 4).

Fig. 5 compares the UBs and the simulated BEPs of the proposed NQSC decoding over AWGN channel for the block length $N = 1024$, the code rate $R = 0.5$, and $Q = q \in \{7, 8\}$. The UBs for odd-level and even-level NQSC decodings are obtained by (17), (20), and (22). The simulated block error probabilities of NQSC decoding for $Q = 8$ and $q = 16, 32$

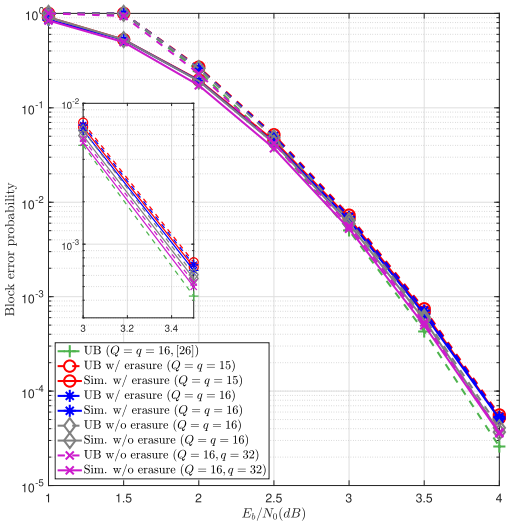

FIGURE 6. UBs and simulated BEPs of uniform-quantized SC decoding [26] and NQSC decoding for $Q = q \in \{15, 16\}$, and $Q = 16$ and $q = 32$ over AWGN channel ($N = 1024$, $R = 0.5$).

are also shown in Fig. 5. For $Q = q = 8$ (3-bit precision quantization), it is confirmed that the proposed asymmetric and symmetric NQSC decoders show about 0.5dB better performance at the BEP 2×10^{-4} compared to the optimized uniform-quantized SC decoder [26]. As expected above, the BEP curves of asymmetric and symmetric 8-level NQSC decoding with and without erasure show a cross point at SNR $= 3.7$dB. Through simulations for $Q = q = 4$ and $Q = q = 8$, the effect of erasure on the performance of NQSC decoding can be summarized as follows.

- As SNR decreases, the effect of erasure increases.
- As the number of quantization levels decreases, the effect of erasure increases.

As shown in Fig. 5, the NQSC decoder for $Q = 8$ and $q = 16, 32$ outperforms the NQSC decoder for $Q = q = 8$ for all SNR range. However, the amount of improvement is smaller than that for the case of $Q = 4$ and there is no further improvement for $Q = 8$ and $q > 16$.

In Fig. 6, the UBs and the BEPs of the proposed NQSC decoding over AWGN channel are compared for the block length $N = 1024$, the code rate $R = 0.5$, and $Q = q \in \{15, 16\}$. The proposed asymmetric and symmetric NQSC decoders show almost the same performance but symmetric one is always slightly better than asymmetric one. This means that there is no erasure effect on the decoding performance for high quantization levels. Also, the error-correction performance of NQSC decoding for $Q = 16$ and $q = 32$ is negligibly improved compared to that for $Q = q = 16$. As the number of quantization levels for quantizer Q increases, the performance improvement of NQSC decoding with $q > Q$ becomes negligible. In Fig. 6, unlike 2- or 3-bit precision quantization, it is shown that for 4-bit precision quantization, the proposed decoding method shows about 0.05dB worse performance at the BEP 4×10^{-5} compared to the optimal uniform-quantized SC decoder [26]. That is because, unlike the optimal uniform-quantized SC decoder,

quantization is not performed for each node and messages take integer values in the proposed decoding method. Specifically, the proposed NQSC decoding has the following advantages in aspects of decoding complexity and memory management compared to the optimal uniform-quantized SC decoding [26].

- In the optimized uniform-quantized SC decoder in [26], quantization is always performed after each check node operation and each repetition node operation, i.e., $N(n+1)$ quantizations should be performed, whereas for the proposed NQSC decoders, additional quantization is not necessary because the quantization values of the quantizer are used.
- In [26], the output values of quantizer, the output message values of each node operation, and the quantized values of uniform-quantized SC decoder are all fixed-point numbers. On the other hand, in the proposed quantization and decoding schemes, the output values of quantizer and the output message values of each node operation are selected from $\mathcal{M}_Q$ and $\mathcal{M}_q$, respectively. That is, only Q and q integers are used in the proposed quantizer and NQSC decoder, respectively. Thus, the proposed quantizer and NQSC decoder require less memory space compared to the uniform quantizer and uniform-quantized SC decoder [26].
- In the optimal uniform-quantized SC decoder in [26], each column of the factor graph consists of 2^s groups and messages of nodes in each group are quantized by one QB value. Since quantization is performed after a codeword is received and after each node operation, $\sum_{i=0}^{n} 2^i$ QB values should be stored, whereas QB values are stored only in the quantizer because quantization is not performed in the proposed NQSC decoder. Therefore, the number of QB values stored in the quantizer is $Q-1$ for both $Q=q$ and $Q<q$. For example, if the block length N is $1024(=2^{10})$ and the number of quantization levels is 16, the uniform-quantized SC decoder [26] needs $2047(=\sum_{i=0}^{10} 2^i)$ QB values, but the proposed NQSC decoder requires only 15 QB values regardless of the block length.

Tables 1, 2, and 3 show the derived QB values $\hat{r}_k$ of $Q=q(=3,4,7,8,15,16)$ and $Q<q$ quantization cases for various E_b/N_0, where w/ 0 and w/o 0 indicate the inclusion and exclusion of erasure, respectively, and $E_c=1$. These QB values are obtained by solving the minimization problems in (17), (20), and (22) through Algorithms 5 and 6. In Algorithm 5, the input parameters are set as $\beta_{\text{ini}}=3$, $\epsilon=0.1$, and $\delta^*=20$. Note that $\hat{r}_{-k}=-\hat{r}_k$ and $\{\hat{r}_{+0},\hat{r}_1,\cdots,\hat{r}_{Q/2-2}\}$ of symmetric even quantization levels are equal to those of symmetric odd quantization levels, e.g., the QB values obtained by Algorithms 5 and 6 are $\{-0.8416,-0.4577,-0.0734,0.0734,0.4577,0.8416,1.3566\}$ when $Q=q=8$, $\gamma=3$dB, and erasure is contained in the quantization levels. As shown in Tables 1, 2, and 3, all QB values decrease as E_b/N_0 increases as expected.

TABLE 1. QB values obtained by Algorithms 5 and 6 for $Q=q=3,4$, and $Q=4$ and $q=8,16,32$ for various SNRs.

(Q,q)	$\hat{r}_k$	E_b/N_0[dB]			
		1	1.5	2	2.5
		3	3.5	4	4.5
		5	5.5	6	6.5
$(3,3)$ w/ 0	$\hat{r}_{+0}$	0.5596	0.5264	0.4975	0.4692
		0.4453	0.4187	0.4035	0.3810
		0.3641	0.3451	0.3300	0.3247
$(4,4)$ w/ 0	$\hat{r}_1$	1.5981	1.5672	1.5186	1.4722
		1.4166	1.3770	1.3320	1.3052
		1.0575	1.0350	1.0156	0.9991
$(4,4)$ w/o 0	$\hat{r}_1$	0.5072	0.4820	0.4607	0.4424
		0.4263	0.4156	0.4006	0.3965
		0.3799	0.3779	0.3675	0.3620
$(4,8)$ w/o 0	$\hat{r}_1$	0.6357	0.6063	0.5816	0.5565
		0.5343	0.5269	0.5256	0.4998
		0.4678			
$(4,16)$ w/o 0	$\hat{r}_1$	0.7564	0.7210	0.6848	0.6493
		0.6046	0.5771	0.5598	0.5243
		0.5035			
$(4,32)$ w/o 0	$\hat{r}_1$	0.7608	0.7246	0.6875	0.6482
		0.6058	0.5779	0.5603	0.5246
		0.5037			

TABLE 2. QB values obtained by Algorithms 5 and 6 for $Q=q=7,8$, and $Q=8$ and $q=16,32$ for various SNRs.

(Q,q)	$\hat{r}_k$	E_b/N_0[dB]			
		1	1.5	2	2.5
		3	3.5	4	4.5
$(7,7)$ w/ 0	$\hat{r}_{+0}$	0.1224	0.1019	0.0876	0.0843
		0.0734	0.0589	0.0506	0.0440
	$\hat{r}_1$	0.5695	0.5398	0.5135	0.4848
		0.4577	0.4310	0.4061	0.3798
	$\hat{r}_2$	1.0341	0.9870	0.9446	0.8916
		0.8416	0.7945	0.7518	0.7087
$(8,8)$ w/ 0	$\hat{r}_3$	1.5587	1.5180	1.4702	1.4157
		1.3566	1.3122	1.2617	1.2146
$(8,8)$ w/o 0	$\hat{r}_1$	0.3540	0.3363	0.3198	0.3041
		0.2829	0.2713	0.2604	0.2569
	$\hat{r}_2$	0.6042	0.5815	0.5568	0.5416
		0.5059	0.4934	0.4862	0.4810
	$\hat{r}_3$	0.9194	0.8900	0.8572	0.8424
		0.7966	0.7819	0.7774	0.7748
$(8,16)$ w/o 0	$\hat{r}_1$	0.4052	0.3827	0.3643	0.3435
		0.3265	0.3137	0.3037	0.2819
	$\hat{r}_2$	0.7770	0.7358	0.7027	0.6636
		0.6306	0.6100	0.5948	0.5631
	$\hat{r}_3$	1.2256	1.1689	1.1243	1.0741
		1.0290	1.0004	0.9870	0.9243
$(8,32)$ w/o 0	$\hat{r}_1$	0.4288	0.4031	0.3812	0.3572
		0.3370	0.3327	0.3110	0.2946
	$\hat{r}_2$	0.8275	0.7796	0.7395	0.6923
		0.6519	0.6272	0.6075	0.5868
	$\hat{r}_3$	1.3055	1.2386	1.1830	1.1198
		1.0630	1.0297	1.0019	0.9735

Especially, in Table 3, it is shown that the boundary values of erasure are 0.0001 close to zero, which means that the quantized SC decoders with erasure for $Q=q=15,16$ have almost no erasure effect. The value 0.0001 indicates the minimum value of QB, i.e., the resolution τ.

Finally, the computational complexity to find the solution of minimization problem is analyzed for Algorithms 4 and 5. Figs 7 and 8 show UBs of BEP according to the number of steps in Algorithms 4 and 5 for the cases of $Q=q=3,5$ and $E_b/N_0=3.5$dB. The slope of UB curve changes either rapidly (elliptical dashed line) or slightly (elliptical solid

TABLE 3. QB values obtained by Algorithms 5 and 6 for $Q = q = 15, 16$, and $Q = 16$ and $q = 32$ for various SNRs.

(Q, q)	$\hat{r}_k$	E_b/N_0[dB]			
		1	1.5	2	2.5
		3	3.5	4	
$(15, 15)$ w/ 0	$\hat{r}_{+0}$	0.0001	0.0001	0.0001	0.0001
		0.0001	0.0001	0.0001	
	$\hat{r}_1$	0.2177	0.2040	0.1873	0.1747
		0.1609	0.1502	0.1422	
	$\hat{r}_2$	0.4665	0.4390	0.4090	0.3796
		0.3556	0.3385	0.3226	
	$\hat{r}_3$	0.7049	0.6648	0.6212	0.5788
		0.5389	0.5190	0.4967	
	$\hat{r}_4$	0.9756	0.9225	0.8621	0.8016
		0.7423	0.7130	0.6804	
	$\hat{r}_5$	1.2774	1.2170	1.1379	1.0639
		0.9910	0.9570	0.9070	
	$\hat{r}_6$	1.5891	1.5273	1.4330	1.3443
		1.2672	1.2366	1.1933	
$(16, 16)$ w/ 0	$\hat{r}_7$	1.8158	1.7402	1.6613	1.5639
		1.4786	1.4606	1.4297	
$(16, 16)$ w/o 0	$\hat{r}_{+0}$	0.1617	0.1549	0.1455	0.1389
		0.1291	0.1208	0.1132	
	$\hat{r}_1$	0.3627	0.3448	0.3302	0.3121
		0.2949	0.2832	0.2725	
	$\hat{r}_2$	0.5523	0.5265	0.5070	0.4796
		0.4528	0.4381	0.4232	
	$\hat{r}_3$	0.7578	0.7243	0.6991	0.6510
		0.6219	0.6005	0.5780	
	$\hat{r}_4$	0.9898	0.9508	0.9220	0.8764
		0.8255	0.7951	0.7611	
	$\hat{r}_5$	1.2399	1.1974	1.1667	1.1163
		1.0607	1.0316	0.9989	
	$\hat{r}_6$	1.5018	1.4568	1.4208	1.3635
		1.3068	1.2827	1.2534	
$(16, 32)$ w/o 0	$\hat{r}_{+0}$	0.1976	0.1838	0.1684	0.1572
		0.1455	0.1315	0.1197	
	$\hat{r}_1$	0.4270	0.4037	0.3770	0.3488
		0.3263	0.3087	0.2904	
	$\hat{r}_2$	0.6509	0.6186	0.5781	0.5343
		0.4992	0.4759	0.4495	
	$\hat{r}_3$	0.9019	0.8606	0.8058	0.7457
		0.6930	0.6561	0.6144	
	$\hat{r}_4$	1.1809	1.1310	1.0649	0.9936
		0.9286	0.8808	0.8185	
	$\hat{r}_5$	1.4787	1.4202	1.3413	1.2572
		1.1860	1.1387	1.0777	
	$\hat{r}_6$	1.7910	1.7338	1.6280	1.5305
		1.4556	1.4094	1.3436	

line), which implies that coarse or fine steps are dominant, respectively. In Figs 7 and 8, it is confirmed that the number of steps η required for $\sum^*$ to converge to the minimum value in Algorithm 5 is smaller than that of Algorithm 4. Specifically, in Algorithm 4 which is an exhaustive search algorithm, the numbers of steps η required to achieve the minimum UB of BEP are $4,187$ for $Q = q = 3$ and $28,513,176$ for $Q = q = 5$, respectively, i.e., it is confirmed that Algorithm 4 has the computational complexity $\mathcal{O}((c/\tau)^{N_r})$ as explained in IV-B2. On the other hand, in Algorithm 5, the minimum values are obtained in 10^2-10^3 steps regardless of β_{ini}. More significantly, as Q increases and τ decreases, it becomes impossible to solve the minimization problem with Algorithm 4, but the proposed iterative C2F search algorithm solves the problem.

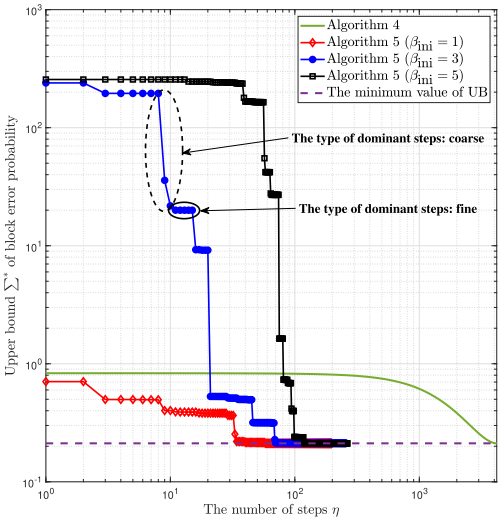

FIGURE 7. UBs $\sum^*$ according to the number of steps η in Algorithms 4 and 5 ($Q = q = 3, E_b/N_0 = 3.5$dB).

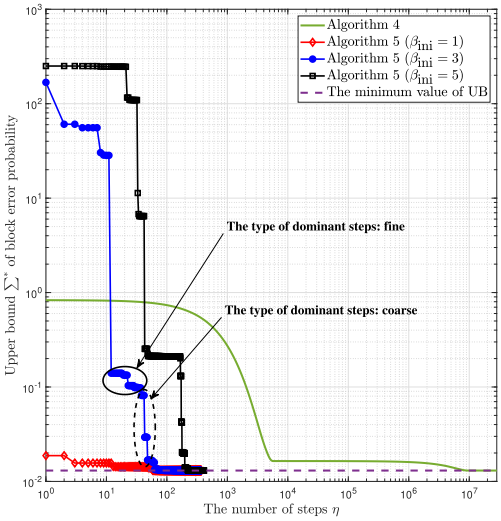

FIGURE 8. UBs $\sum^*$ according to the number of steps η in Algorithms 4 and 5 ($Q = q = 5, E_b/N_0 = 3.5$dB).

VI. CONCLUSION AND DISCUSSION

In this paper, an effective NQM and NQSC decoding algorithm for polar codes are proposed over AWGN channels. By deriving an UB of BEP through density evolution analysis and minimizing this UB with respect to QB variables, both QB values and the information set $\mathcal{I}$ are obtained. Since this minimization problem cannot be solved with trivial search algorithms, we propose an iterative C2F search algorithm to solve it. Through simulations, it is verified that the proposed iterative C2F search algorithm is able to solve the complicated minimization problem with low computational complexity.

Through simulations, for $2, 3$-bit precision quantization, it is confirmed that the proposed method outperforms the existing best quantization method in [26]. Although the proposed decoding method shows a slight degradation in error-correction performance compared to the optimal uniform-quantized SC decoder in [26] for 4-bit precision

quantization due to the difference between these two decoding methods as explained in V, the proposed method has advantages such as low decoding complexity and high memory efficiency.

Moreover, in various communication and memory systems, the proposed NQSC decoding method for $Q < q$ can reduce the decoding latency and the number of sensing operations without noticeable error-correction performance degradation. Specifically, the average decoding latency can be further reduced by performing decoding with low quantization levels ($Q = q$) and repeating decoding after increasing the number of quantization levels of quantized SC decoder ($Q < q$) only when decoding fails. Additionally, in memory systems, decoding requires soft information that demands fine-grained threshold-voltage sensing operation [22] and hence incurs energy consumption and access latency penalty. Therefore, it is important to minimize the number of threshold-voltage sensing operations without serious degradation of error-correction performance. The number of threshold-voltage sensing operations is proportional to the number of quantization levels Q for quantizer. If the proposed NQSC decoding method for $Q < q$ is applied to memory systems, it is possible to reduce the number of threshold-voltage sensing operations ($\propto Q$) without noticeable error-correction performance degradation.

REFERENCES

[1] E. Arikan, "Channel polarization: A method for constructing capacity-achieving codes for symmetric binary-input memoryless channels," *IEEE Trans. Inf. Theory*, vol. 55, no. 7, pp. 3051–3073, Jul. 2009.
[2] N. Hussami, S. B. Korada, and R. Urbanke, "Performance of polar codes for channel and source coding," in *Proc. IEEE Int. Symp. Inf. Theory*, Jun. 2009, pp. 1488–1492.
[3] I. Tal and A. Vardy, "List decoding of polar codes," *IEEE Trans. Inf. Theory*, vol. 61, no. 5, pp. 2213–2226, May 2015.
[4] K. Chen, K. Niu, and J. R. Lin, "List successive cancellation decoding of polar codes," *Electron. Lett.*, vol. 48, no. 9, pp. 500–501, Apr. 2012.
[5] K. Niu and K. Chen, "Stack decoding of polar codes," *Electron. Lett.*, vol. 48, no. 12, pp. 695–696, Jun. 2012.
[6] C. Leroux, I. Tal, A. Vardy, and W. J. Gross, "Hardware architectures for successive cancellation decoding of polar codes," in *Proc. IEEE Int. Conf. Acoust., Speech Signal Process. (ICASSP)*, May 2011, pp. 1665–1668.
[7] C. Leroux, A. J. Raymond, G. Sarkis, and W. J. Gross, "A semi-parallel successive-cancellation decoder for polar codes," *IEEE Trans. Signal Process.*, vol. 61, no. 2, pp. 289–299, Jan. 2013.
[8] Y. Fan and C.-Y. Tsui, "An efficient partial-sum network architecture for semi-parallel polar codes decoder implementation," *IEEE Trans. Signal Process.*, vol. 62, no. 12, pp. 3165–3179, Jun. 2014.
[9] A. J. Raymond and W. J. Gross, "A scalable successive-cancellation decoder for polar codes," *IEEE Trans. Signal Process.*, vol. 62, no. 20, pp. 5339–5347, Oct. 2014.
[10] K. Niu and K. Chen, "CRC-aided decoding of polar codes," *IEEE Commun. Lett.*, vol. 16, no. 10, pp. 1668–1671, Oct. 2012.
[11] A. Balatsoukas-Stimming, M. B. Parizi, and A. Burg, "LLR-based successive cancellation list decoding of polar codes," *IEEE Trans. Signal Process.*, vol. 63, no. 19, pp. 5165–5179, Oct. 2015.
[12] *Polar Code Construction for NR*, document R1-1608862, 3GPP TSG RAN WG1 Meeting, Huawei, HiSilicon, Oct. 2016.
[13] *Technical Specification Group Radio Access Network; NR, Multiplexing and Channel Coding (Release 15)*, document TS 38.212, 3GPP, Dec. 2017.
[14] L. Xiang, Z. B. K. Egilmez, R. G. Maunder, and L. Hanzo, "CRC-aided logarithmic stack decoding of polar codes for ultra reliable low latency communication in 3GPP new radio," *IEEE Access*, vol. 7, pp. 28559–28573, Feb. 2019.
[15] P. Chen, B. Bai, Z. Ren, J. Wang, and S. Sun, "Hash-polar codes with application to 5G," *IEEE Access*, vol. 7, pp. 12441–12455, Jan. 2019.
[16] H. Wang, X. Tao, N. Li, and H. Wu, "Polar coding for the multiple access channel with confidential messages," *IEEE Access*, vol. 8, pp. 3416–3426, Dec. 2019.
[17] Y. Li, K. Niu, and C. Dong, "Polar-coded GFDM systems," *IEEE Access*, vol. 7, pp. 149299–149307, Oct. 2019.
[18] R. S. Zakariyya, K. H. Jewel, A. O. Fadamiro, O. J. Famoriji, and F. Lin, "An efficient polar coding scheme for uplink data transmission in narrowband Internet of Things systems," *IEEE Access*, vol. 8, pp. 191472–191481, Oct. 2020.
[19] X. Wang, T. Wang, J. Li, and Y. Zhang, "Improved multiple bit-flipping fast-SSC decoding of polar codes," *IEEE Access*, vol. 8, pp. 27851–27860, Jan. 2020.
[20] H. Song, C. Zhang, S. Zhang, and X. You, "Polar code-based error correction code scheme for NAND flash memory applications," in *Proc. 8th Int. Conf. Wireless Commun. Signal Process. (WCSP)*, Oct. 2016, pp. 1–5.
[21] L. Kong, Y. Liu, H. Liu, and S. Zhao, "Protograph QC-LDPC and rate-adaptive polar codes design for MLC NAND flash memories," *IEEE Access*, vol. 7, pp. 37131–37140, Mar. 2019.
[22] S. Qi, D. Feng, and J. Liu, "Optimal voltage signal sensing of NAND flash memory for LDPC code," in *Proc. IEEE Workshop Signal Process. Syst. (SiPS)*, Oct. 2014, pp. 1–6.
[23] S. H. Hassani and R. Urbanke, "Polar codes: Robustness of the successive cancellation decoder with respect to quantization," in *Proc. IEEE Int. Symp. Inf. Theory*, Jul. 2012, pp. 1962–1966.
[24] J. Neu, M. C. Coskun, and G. Liva, "Ternary quantized polar code decoders: Analysis and design," in *Proc. 53rd Asilomar Conf. Signals, Syst., Comput.*, Nov. 2019, pp. 1724–1728.
[25] S. Aizaz A. Shah, M. Stark, and G. Bauch, "Design of quantized decoders for polar codes using the information bottleneck method," in *Proc. IEEE Int. ITG Conf. Syst., Commun., Coding (SCC)*, Mar. 2019, pp. 1–6.
[26] Z. Shi, K. Chen, and K. Niu, "On optimized uniform quantization for SC decoder of polar codes," in *Proc. IEEE 80th Veh. Technol. Conf. (VTC-Fall)*, Sep. 2014, pp. 1–5.
[27] S. Zhao, P. V. Rengasamy, H. Zhang, S. Bhuyan, N. C. Nachiappan, A. Sivasubramaniam, M. T. Kandemir, and C. Das, "Understanding energy efficiency in IoT app executions," in *Proc. IEEE 39th Int. Conf. Distrib. Comput. Syst. (ICDCS)*, Jul. 2019, pp. 742–755.
[28] U. U. Fayyaz and J. R. Barry, "Low-complexity soft-output decoding of polar codes," *IEEE J. Sel. Areas Commun.*, vol. 32, no. 5, pp. 958–966, May 2014.
[29] T. J. Richardson and R. L. Urbanke, "The capacity of low-density parity-check codes under message-passing decoding," *IEEE Trans. Inf. Theory*, vol. 47, no. 2, pp. 599–618, Feb. 2001.
[30] R. Mori and T. Tanaka, "Performance and construction of polar codes on symmetric binary-input memoryless channels," in *Proc. IEEE Int. Symp. Inf. Theory*, Jun. 2009, pp. 1496–1500.
[31] K. Pearson, "The problem of the random walk," *Nature*, vol. 72, no. 1865, p. 294, Jul. 1905, doi: 10.1038/072294b0.

JIHO KIM (Member, IEEE) received the B.S. degree in electronics and communication engineering from Hanyang University, Seoul, South Korea, in 2013, where he is currently pursuing the Ph.D. degree in electronics and computer engineering. His research interests include signal processing, error-correcting codes, and artificial intelligence.

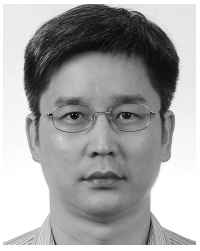

DONG-JOON SHIN (Senior Member, IEEE) received the B.S. degree in electronics engineering from Seoul National University, Seoul, South Korea, the M.S. degree in electrical engineering from Northwestern University, Evanston, USA, and the Ph.D. degree in electrical engineering from the University of Southern California, Los Angeles, USA. From 1999 to 2000, he was a Member of Technical Staff with Wireless Network Division and Satellite Network Division, Hughes Network Systems, Germantown, MD, USA. Since September 2000, he has been with the Department of Electronic Engineering, Hanyang University, Seoul. His current research interests include signal processing, error-correcting codes, artificial intelligence, and cryptography.